A Reliable Multiple Access Scheme Based on Chirp Spread Spectrum and Turbo Codes

by

Aida Arman Moghadam

A thesis
presented to the University of Waterloo
in fulfillment of the
thesis requirement for the degree of
Master of Science
in
Electrical and Computer Engineering

Waterloo, Ontario, Canada, 2017

I hereby declare that I am the sole author of this thesis. This is a true copy of the thesis, including any required final revisions, as accepted by my examiners.

I understand that my thesis may be made electronically available to the public.

Abstract

Nowadays, smart devices are the indispensable part of everyone's life and they play an important role in the advancement of industries and businesses.These devices are able to communicate with themselves and build the super network of the Internet of Things(IoT). Therefore, the need for the underlying structure of wireless data communications gains momentum. We require a wireless communication to support massive connectivity with ultra-fast data transmission rate and ultra-low latency. This research explores two possible methods of tackling the issues of the current communication systems for getting closer to the realization of the IoT. First, a grant-free scheme for uplink communication is proposed. The idea is to the combine the control signals with data signals by superimposing them on top of each other with minimal degradation of both signals. Moreover, it is well-established that orthogonal multiple access schemes cannot support the massive connectivity. Ergo, the second part of this research investigates a Non-Orthogonal Multiple Access(NOMA) scheme that exploits the powerful notion of turbo codes for separating the signals in a slow fading channel. It has been shown that in spite of thesimplicity of the design, it has the potentials to surpass the performance of Sparse Code Multiple Access(SCMA) scheme.

Acknowledgements

First and foremost, I would like to express my utmost admiration and sincere gratitude to my supervisor, Professor Amir Keyvan Khandani, for his great supervision. It has been a great honor to work with him, and I wish to take this opportunity to thank him for his effort, care, and guidance.

I would like to especially acknowledge my dear friend Neda Mohammadizadeh and Ehsan Seifi for their collaboration on this research and also for their friendship and constant support.

Finally, I would like to extend my deepest gratitude, love, and affection to my beloved parents, Mehrnaz and Alireza, and my sister Dorsa, who supported me throughout the long path of my academic endeavor and endured countless sacrifices so that I can have the absolute best education. To them, I owe all I have ever accomplished.

Table of Contents

List of Tables

List of Figures

Abbreviations

APP A Posteriori Probability 38

AWGN Additive White Gaussian Noise viii, 11, 22, 23, 26, 49, 50

BCH Bose-Chaudhuri-Hocquenghem 4, 25, 29

BCJR Bahl, Cocke, Jelinek, Raviv 25, 38

BER Bit Error Rate viii, 11–13, 35, 36, 42, 48, 50

BLER Block Error Rate 35, 48–50, 52

BOK Binary Orthogonal Keying viii, 10, 11, 13

BPSK Binary Phase Shift Keying 4, 27, 30, 47

CDMA Code Division Multiple Access ix, 2, 32–34

CSS Chirp Spread Spectrum viii, 7, 10, 11, 13, 22, 23

DCI Downlink Control Information 6, 25

FDMA Frequency Division Multiple Access 1, 33

FEC Forward Error Correction 25, 28

FSK Frequency Shift Keying viii, 8, 10

Chapter 1

Introduction

Nowadays, smart devices are the indispensable part of everyone's life and they play an important role in the advancement of industries and businesses.This devices are able to communicate with themselves and they build the super network of the Internet of Things (IoT). Therefore, the need for the underlying structure of wireless data communications gains momentum. We are requiring a wireless communication to support massive connectivity with the ultra fast data transmission rate and ultra low latency. These requirements cannot be addressed by current communication systems. For example, the grant-based nature of LTE uplink fails to support massive connectivity or ultra low latency specifications. In addition, the cost of control signaling overhead, latency, and energy efficiency are prominent challenges in IoT applications.

In this thesis, we are proposing a grant-free scheme for transmission of control and data signals over shared time/frequency resources by exploiting the potentials of spread spectrum communication systems. We will use a chirp signal for modulation of the low rate control data and then it will be superimposed on top of the information signal with minimal degradation. A chirp signal, similar to other spread spectrum systems, uses the entire allocated bandwidth to broadcast the signal and it has the inherent capability of interference attenuation.

While the preceding generations of communication systems exploited the Frequency Division Multiple Access (FDMA) in 1G, Time Division Multiple Access (TDMA) in 2G,

CDMA in 3G and Orthogonal Frequency Division Multiple Access (OFDMA) for 4G, Non-Orthogonal Multiple Access (NOMA) is one of the approaches proposed for 5G to tackle the limitations of the preceding schemes by allowing deliberate interference in the system. By elimination of the orthogonality requirement of LTE, NOMA is able to achieve multiuser capacity both in uplink and downlink. Being resistant to the multiuser interference is another feature of NOMA, enabling it to support longer connections with a performance near to the single user communication. Easier scheduling and link adaptation for mobile users via grant-free transmission can also be counted as the functionalities of NOMA.

From the theoretical point of view, Shannon proved that there exist ideal error-correcting codes that allow data to be transmitted error-free when the rate is less than the maximum capacity of a communication channel. Nevertheless, Shannons work imposed the unanswered question of constructing the idea channel codes. The sophisticated algebraic constructions of channel codes failed to achieve what the theory promised. When the turbo codes were introduced, it was proved that they are able to achieved rates with a minuscule gap to its capacity. In turbo codes, two or more component codes are used, and decoding involves feeding outputs from one decoder to the inputs of other decoders in an iterative fashion. In fact, the soft information on data bits passed between the components of the turbo codes and then they would be fed back again at the beginning to increase the reliability of the decisions. The notion of the iterative passing of soft information between components of the system become a valuable asset in communication systems since then. In this thesis, a NOMA scheme is used in conjunction turbo code. We will be using the iterative message passing notion of turbo codes to decode the data signals of multiple sources superimposed on top of each other.

1.1 Problem Formulation

At the current communication systems, the control and data signals are transmitted over separate time/frequency resources. Since the control signal information has a very small size (of the order of bits or tens of bits), it requires small Signal-to-Noise Ratio (SNR) to be decoded. This means that one can superimpose the control over data with proper

power allocation to assure the control signal decoding satisfies the requirements. It will save the control overhead dramatically, especially when the number of symbols in the slot is small (like mini-slot configurations in which each OFDMA slot can have as small as 2 symbols, which is working assumption for phase 1 of New Radio for 5G (NR)). Note that, in the traditional way of sending Physical Downlink Control CHannel (PDCCH), we are dedicating 3 symbols (out of 14) for control. However, when we have only 2 symbols per slot, we cannot afford to allocate 1 symbol to control as it implies large overhead. The purpose of the first part of the study is to show:

- The idea works, i.e. when we are superimposing the data and control, we can guarantee the required reliability for both control and data. Typically, the reliability requirement for control is higher than data. In other words, we have to show we do not see any error floor when we do the superimposing.

- Show that we can have a performance superior to that of the traditional systems.

In addition, we are seeking for a reliable and efficient communication system for transmission of the information signals coming from different sources. We need a system with following specifications

- Good spectral efficiency

- Low latency

- Simple and low-cost decoding

Chapter 2

Sending control Information as superimposed data layer

In this chapter, the focus is on proposing a grant-free scheme for transmission of control data and information data. Since we are dealing with small packets in IoT, we cannot afford to dedicate septate frequency/time resources for control signaling. The idea is to use chirp spread spectrum for superimposing control data on top of the information data, using the same time and frequency resources. First, we will review the current control signaling scheme used in LTE. Then we will go over the concepts of spread spectrum and chirp spread spectrum as a proposed modulation scheme.

In addition, a survey on slow fading channels is also included. It is because of the fact that chirp signals will experience time-variant fading due to longer durations of such signals. The simulation results of the slow fading channels are included in this chapter. Then, we investigated the idea of superimposition of side information on top of the data signal with Binary Phase Shift Keying (BPSK) modulation and Bose-Chaudhuri-Hocquenghem (BCH) channel coding scheme. It has been shown that we will be able to achieve better rates for high ranges of SNR by using superimposition scheme compared with the conventional method of transmitting control signals.

2.1 Review of Control Signaling in Current Communication Systems

Every multiple access system require a control signaling scheme to facilitate communication between a transmitter and a receiver. This is because of the fact that the users need the transmission parameters prior to the actual payload in order to decode the information successfully. Therefore, any practical system requires a technique to allocate resources to control signals efficiently.

OFDMA is multiple access scheme of LTE in which the data symbols of each user are spread over a specific frequency band. In this scheme, each subcarrier is orthogonal to the others and carries the information data of one specific user.The underlying data carrier for a LTE frame is the Resource Element (RE) and it is the smallest discrete part of the frame and contains a single complex value representing data from physical channel. The physical layer channel resource of LTE is illustrated in figure 2.1.
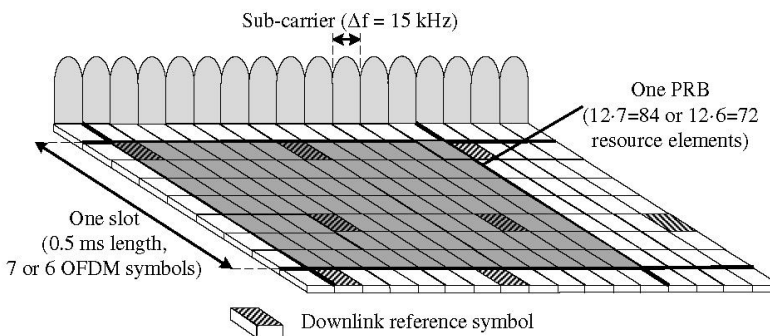
Figure 2.1: LTE physical layer channel resources [2]

Orthogonal Frequency Division Multiplexing (OFDM) is the orthogonal scheme used in LTE for both uplink and downlink. OFDMA is

In LTE structure, the control data information is embedded in the beginning of the each subframe in the form of Resource Block (RB) pairs containing two REs. The number of RBs allocated to the control signaling varies depending on the channel traffic for reducing

the signaling overhead whenever it is possible. For example, when there are many users with data to be transmitted, three OFDM symbols are used for control signaling. On the other hand, when there is a small number of them with data, only one OFDM symbol will be used. Then, the payload is transmitted in the form of transport blocks. The reason for placing control data information at the beginning is that a receiver needs to obtain information about the resource allocation and the transmission parameters as soon as possible. Otherwise, a terminal should wait until the entire subframe is received to start the decoding process. The control region of the LTE consists of three different physical channel type:

1. **Physical Control Format Indicator Channel** This channel is used to signal the size of the control region. If a terminal fails to decode the information of this channel, it neither knows where to look for the control data nor where does the information data start.

2. **Physical Hybrid Automatic Repeat Request (HARQ) Indicator Channel**: This channel carries the HARQ acknowledgment response to the uplink data transmission.

3. **PDCCH**: This channel is used to send Downlink Control Information (DCI), which contains downlink scheduling assignments, information about the format of the transport block, control information about the spatial multiplexing. DCI can be of different sizes depending on its format.

2.2   Spread Spectrum Principles

Spread spectrum communication has the inherent interference attenuation capability and it has many diverse applications since very early communication systems. Basically, in spread spectrum systems, the occupied bandwidth is sacrificed for gaining a plenitude of benefits such as anti-jamming and the resistance toward the interference.

A signal set can always be decomposed to a linear combination of M auto-normal basis

functions. Although the white noise requires an infinite number of bases, only the terms within the signal space are effective.

The rationale behind the benefits of spread spectrum communication is that when we are disturbing a low-dimensional data signal in a higher dimension, a fixed power interference can either induce a little interference over all of the dimensions or it can place all of the power into a relatively small subspace and leave the rest untouched [32].

According to the Shannon-Hartley theorem, the maximum rate at which information can be transmitted over a noisy communication channel with the bandwidth B is

$$C = B * log_2(1 + SNR) \tag{2.1}$$

where C is the channel capacity. Note that for spread spectrum applications the signal to noise ratio is small since the signal power is often below the noise floor. Assuming a noise level such that $S/N << 1$, we can use the $ln(1 + x) = x$ for small values of x; Hence, we can rewrite the equation as follows

$$\frac{C}{B} = 1.433 * SNR \tag{2.2}$$

It means that increasing the bandwidth of the channel can help us to transmit error free information.

2.2.1 Chirp Spread Spectrum

In IoT, we are specifically interested in the transmission of small packets under the constrained energy with fixed amount of bandwidth. Due to regulatory constraints, it is necessary to share the bandwidth with conventional systems, for example, LTE, while adding only minimal interference to these other types of transmissions. CSS modulation which trades rate for sensitivity is a suitable candidate to meet these requirements. This modulation uses chirp for signal transmission and matched filter for extracting the embedded information.

A chirp is a signal in which the frequency changes over time. Similar to other spread spectrum methods, chirp signal utilizes the entire allocated bandwidth to broadcast the

signal. The spectral efficiency of chirp is signals is compared against that of an FSK in figure 2.2 and 2.3. In addition, chirp signals can be easily implemented using Surface Acoustic Wave (SAW) chirped delay lines. The key features of chirp spread spectrum can be summarized as follows:

1. Sharing the frequency bandwidth with many types conventional transmission with minimal interference

2. Substantial resistance to a narrow-band interference

3. Multipath and fading resistance

4. Low power constant envelope

5. Receiver with low complexity

The theory of chirp signals

A signal with chirp waveform and the duration T, can be written as

$$s(t) = a(t)cos(\Theta(t)) \tag{2.3}$$

where $a(t)$ is the envelope of the signal and it is zero, except for the duration T. In addition, $\Theta(t)$ is the phase of signal, from which we can extract the instantaneous frequency and the chirp rate as

$$f_M(t) = \frac{1}{2\pi}\frac{d\Theta}{dt} \tag{2.4}$$

and,

$$\mu(t) = \frac{df_M}{dt} = \frac{1}{2\pi}\frac{d^2\Theta}{dt^2} \tag{2.5}$$

Now we can define up-chirps and down-chirps as the waveforms with $\mu(t) > 0$ and $\mu(t) < 0$, respectively. Furthermore, in the linear chirp waveforms the frequency changes linearly with t, so the chirp rate is constant. Such chirp waveform can be written as

$$s(t) = a(t)cos[2\pi f_c t + \pi\mu t^2 + \phi_0] \tag{2.6}$$

8
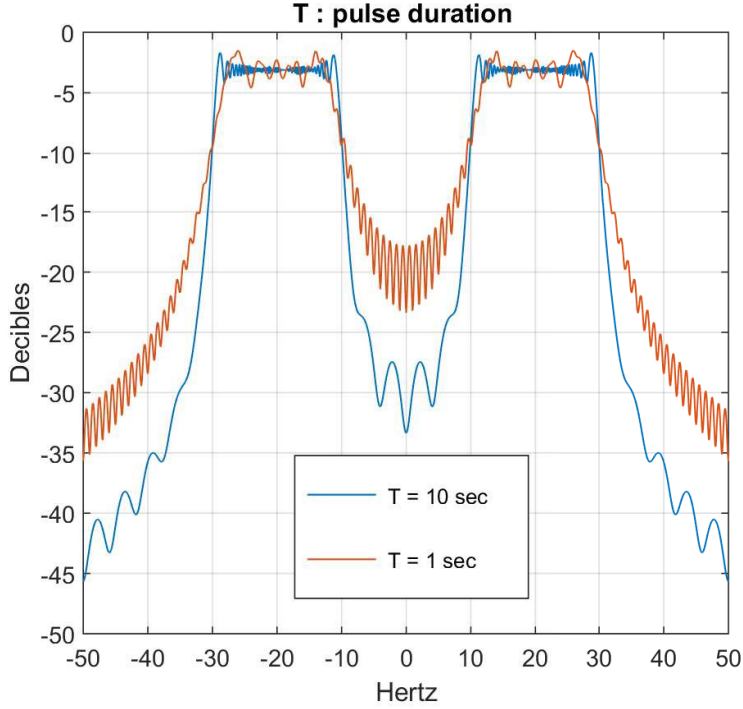
Figure 2.2: Chirp signals spectral density

where f_c is the center frequency and $a(t) = 0$ for $|t| > T/2$. The bandwidth B is defined to be the range of the instantaneous frequency, so that

$$B = |\mu|T \qquad (2.7)$$

If we want to use linear chirp waveforms, we are required to use a matched filter for detection. The impulse response of a matched filter for a linear chirp signal is again a linear chirp signal with an opposite sign chirp rate. The analytical expression for the output waveform $g(t)$ of the matched filter which is centered at $t = 0$ is

$$g(t) = h(t) * s(t) = \phi_{ss}(t) \qquad (2.8)$$

where ϕ_{ss} is the autocorrelation function of $s(t)$ and for the $-T < t < T$; thus, it can be written as

$$\phi_{ss}(t) = \sqrt{BT} \frac{sin(\pi Bt(1 - \frac{|t|}{T}))}{\pi Bt} cos(2\pi f_c t) \qquad (2.9)$$

9
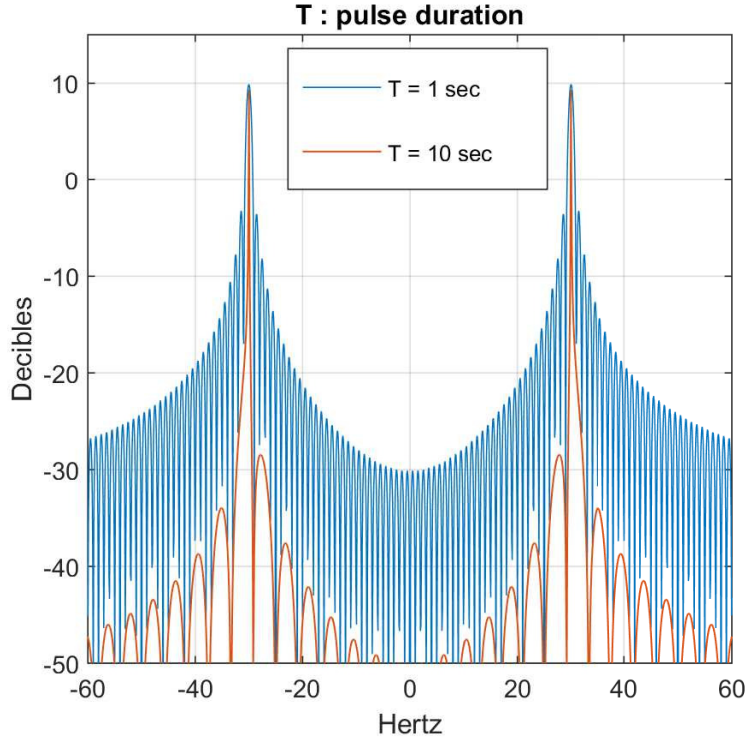
Figure 2.3: FSK signal spectral density

It has its maximum at $t = 0$, and its first zeros at $t \approx \pm BT$. Then, the ratio of the input and output pulse width can be given by the time-bandwidth product and it will be used afterward as compression rate or processing gain, as a measure for the quality of detection of the chirp signal waveforms.

Binary orthogonal keying with chirp signals

We can assume that the up-chirp and down-chirp signals are roughly orthogonal. Therefore, they can be used in BOK modulation such that '1' stimulates an up-chirp signal and '0' stimulates a down-chirp signal, and vice versa. For example, the following signals can be used for the BOK-CSS modulation.

$$up - chirp: \quad s_0 = cos((2\pi f_c + \pi\mu t)t) \quad \frac{-T}{2} \le t \le \frac{T}{2} \tag{2.10}$$

$$down - chirp: \quad s_0 = cos((2\pi f_c - \pi\mu t)t) \quad \frac{-T}{2} \leq t \leq \frac{T}{2} \quad (2.11)$$

As it is mentioned before, the orthogonality of chirp signals significantly affects the performance of BOK-CSS systems in terms of the BER. Obviously, the better orthogonality will lead to a superior performance. Due to the fact that these signals are not exactly orthogonal, a disturbing cross-correlation occurs in matched filters, preventing the system to achieve the theoretical BER of a BOK system. Figure 2.4 depicts how linear chirp signals frequency changes over time for parameters $f_c = 20Hz$, $\mu = 20Hz/s$ and $T = 1s$.
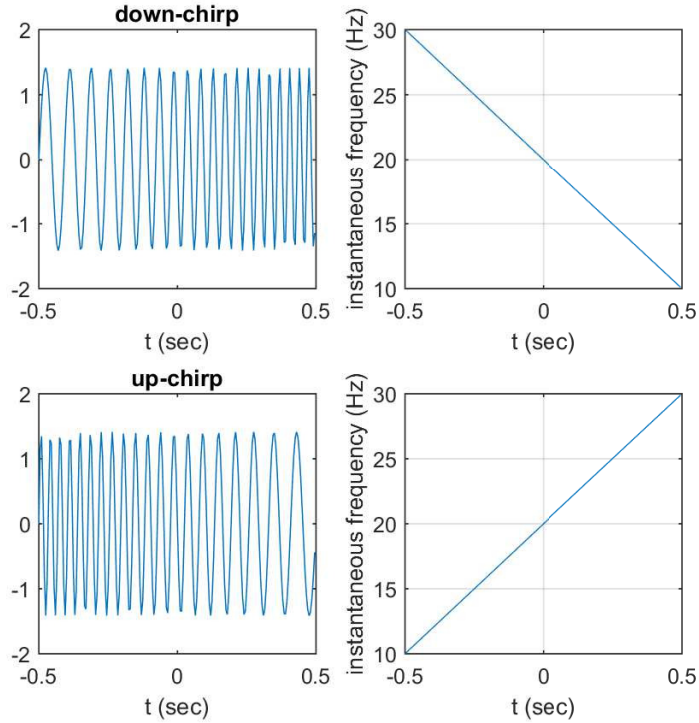
Figure 2.4: BOK-CSS signals

The time bandwidth product BT of a signal set can be a good measure for determining the orthogonality of the signals. Figure 2.5 illustrates such relations.

Moreover, the relationship between BER performance of the BOK-css systems in AWGN
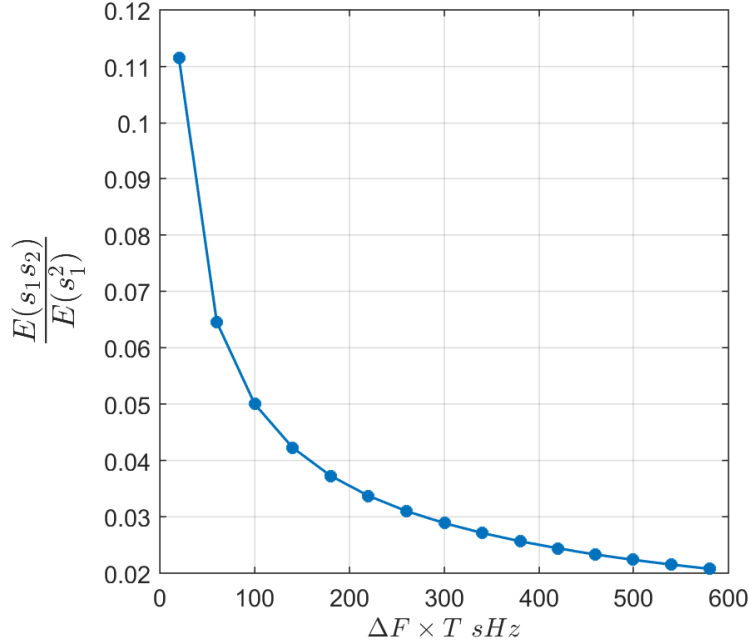
Figure 2.5: Cross-correlation between up-chirp and down-chirp signals as a function of time-bandwidth product

channel and ρ (or likewise $T.\Delta F$) is depicted in the figure 2.6. It can be seen that when ρ is close enough to zero, meaning that the two chirps are quasi-orthogonal, the best BER performance is achieved.

2.3   Fast fading channel model

When we want to send an information signal in a wireless communication channel, we should deal with a numerous phenomena such as multipath and shadowing. One way to tackle the problem is to know what is exactly happening in the channel, meaning that we can use an exact mathematical model to describe the effective factor. However, the fact is that the communication channels are too complex to be modeled easily. In other words, precise model of a channel might be either unknown or too complex for considering it for

Figure 2.6: BER perfromance of BOK-CSS

system analysis. Thus, we should find a practical alternative. Fortunately, there exists a range of relatively straightforward and practically accurate statistical models. Simulation of the wireless fading channel requires multiple mutually independent Rayleigh fading correlated samples whose correlation property is related to maximum Doppler shift. We define the coherent bandwidth of a channel to be the bandwidth in which the input signal does not experience distortion. Then the channel is said to be frequency selective if the coherent bandwidth of the channel is smaller than the bandwidth of the transmitted signal. If the transfer function of a channel is also time-variant, it will add to the complexity of the model. All in all, the multipath Rayleigh fading channel can be modeled with a tapped delay line transversal filter with time variant tap coefficients [46].

When a signal is experiencing fading, both its envelope and phase fluctuates over time. In the case of coherent modulations, phase distortion resulted by the fading, severely

degrade the performance of the system. However, we are usually able to compensate for the phase distortion by using the measurements of the channel. On the other hand, non-coherent modulations do not require the phase information and the phase distortions can be ignored. Thus, the performance analysis of the communication systems for either coherent or non-coherent modulation requires only the knowledge of envelopes of the information signals.

Many different techniques have been proposed to simulate the wireless channels. They generate uncorrelated fading waveforms for the modeling the frequency selective fading channels as well as the Multiple Input Multiple Output (MIMO) channels. Each of them is able to successfully model the channel for some specific applications while having drawbacks that make it unusable in other cases. Rayleigh and Rician fading channels are able to successfully model the real-world phenomena in wireless communication systems.

In the presence of some buildings in the environment, signals will experience reflection, leading to the arrival of the delayed versions of them at the receiver. Moreover, the signal of each major path faces local scattering because of the reflections by obstacles near the receiver. The combination of these phenomena at the receiver causes multipath fading. Meaning that each major path acts as a single fading path. Rayleigh distribution can be exploited to model non-line-of-sight paths and a Rician distribution for a line-of-sight path. Furthermore, if the receiver has a relative motion to the transmitter, Doppler shift happens. Due to the fact that the scattering happens in many angles, we face a range of Doppler shifts, also known as Doppler spectrum. The maximum Doppler shift in the spectrum obviously corresponds to the component whose direction is the opposite of the receiver's trajectory. For the modeling purposes, we assume that there are N fading paths with their own delay and average power. When there is only one path, i.e. $N = 1$ the channel is said to be frequency flat; otherwise, it is called a frequency selective channel, given the signal's bandwidth is sufficiently wide. For each major path, Rayleigh model is assumed with Jake Doppler spectrum.

A well-known model for a discrete multipath channel is TDL channel model [46]. In the TDL model, the low pass impulse response of the channel is modeled as

$$\tilde{c}(\tau(t), t) = \sum_{k=1}^{K(t)} \tilde{a}_k(\tau_k(t), t)\delta(\tau - \tau_k(t)) \tag{2.12}$$

where $K(t)$ is the number of path, which is assumed to be time variant, $\tilde{a}_k(\tau_k(t), t)) = a_k(t)e^{-j2f_c\tau_k(t}$ are the low-pass time-varying complex channel coefficients, $\tau_k(t)$ are the time-varying delays, f_c is the carrier frequency. We can simplify the above equation by time-invariant assumption to

$$\tilde{c}(t, \tau) = \sum_{k=1}^{K} \tilde{a}_k(\tau_k, t)\delta(\tau - \tau_k) \tag{2.13}$$

If the $\tilde{s}(t)$ is a lowpass input to a TDL channel. Then, the lowpass output $y(t)$ is obtained as the convolution between the input and the impulse response:

$$\tilde{y}(t) = \tilde{s}(t) * \tilde{c}(t, \tau) = \sum_{k=1}^{K} \tilde{a}_k(\tau_k, t)\tilde{s}(\tau - \tau_k) \tag{2.14}$$

A TDL channel model can be illustrated as Figure 2.7
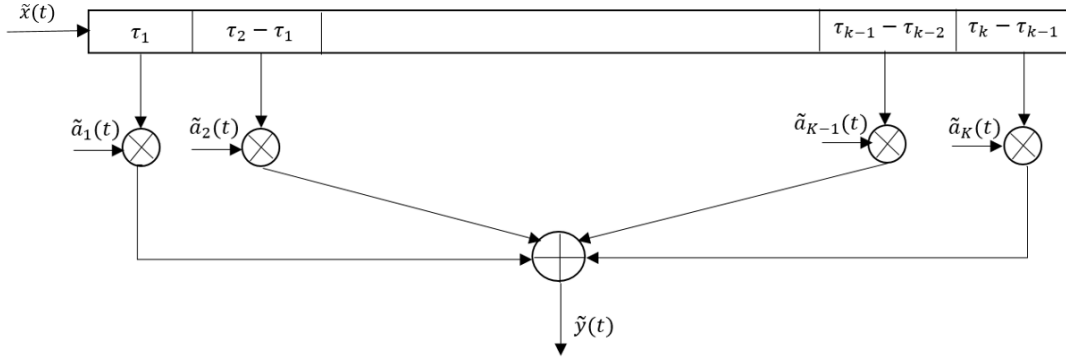
Figure 2.7: TDL channel model

There is another method with less accuracy but faster simulation speed by employing a bandlimited discrete channel model. In this method, it is assumed that the input of the

15

channel is bandlimited to a bandpass bandwidth B. Hence, it can be expressed as:

$$\tilde{s}(t - \tau) = \sum_{n=-\infty}^{\infty} \tilde{s}(t - nT_s)sinc(B(\tau - nT_s)) \tag{2.15}$$

Then the lowpass signal of the output is

$$\tilde{y}(t) = \sum_{n=-\infty}^{\infty} \tilde{s}(t - nT_s)\tilde{g}_n(t) \tag{2.16}$$

where

$$\tilde{g}_n(t) = \sum_{k=1}^{K} \tilde{a}_k(t)sinc(B(\tau_k - nT_s)) = \sum_{k=1}^{K} \tilde{a}_k(t)\alpha(k,n) \tag{2.17}$$

In which

$$\alpha(k,n) = sinc(B(\tau_k - nT_s)) = sinc(\tau_k/T_s - n) \tag{2.18}$$

Practically, we do not need all of the terms. Thus, the convolution sum can be truncated to a finite number of terms. One approach to truncation is to set a threshold such that tap-gain processes having a set of coefficients less than that threshold are discarded. The discrete-time implementation of the above equation with the sampling period T_s, can be expressed as:

$$\tilde{y}[i] = \sum_{n=-N_1}^{N_2} \tilde{s}[i - n]\tilde{g}_n[i] \tag{2.19}$$

where $\tilde{s}[i] = \tilde{s}(iT_s)$ and $\tilde{g}_n[i] = \tilde{g}_n(iT_s)$. Figure 2.8 depicts the TDL of this model.

For a block of N samples, the above equation can be put in the matrix form as:

$$\tilde{y} = \sum_{columns} \tilde{g}. * U \tag{2.20}$$

With .* denoting the element-wise matrix multiplication, and

$$\tilde{g} = \alpha \times \tilde{a} \tag{2.21}$$

where

$$\alpha = \begin{bmatrix} \alpha(1, -N_1) & \cdots & \alpha(K, -N_1) \\ \vdots & \ddots & \vdots \\ \alpha(1, N_2) & \cdots & \alpha(K, N_2) \end{bmatrix} \tag{2.22}$$

16
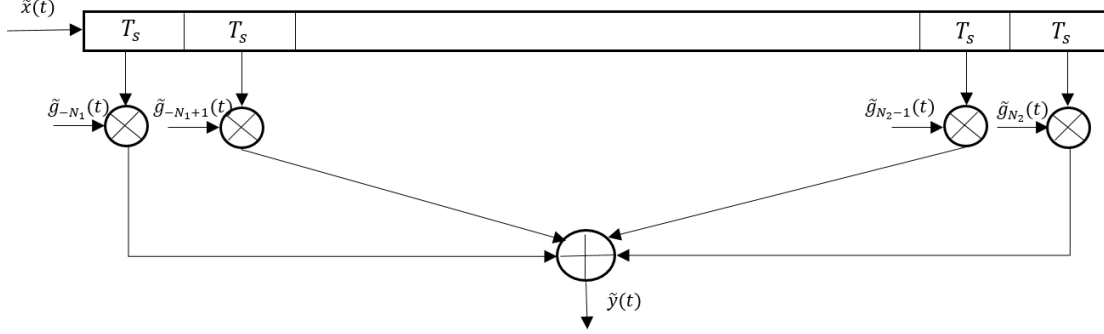
Figure 2.8: TDL channel model

And,

$$\tilde{a} = \begin{bmatrix} \tilde{a}(1) & \cdots & \tilde{a}(N) \\ \vdots & \ddots & \vdots \\ \tilde{a}(1) & \cdots & \tilde{a}(N) \end{bmatrix} \tag{2.23}$$

Also

$$U = \begin{bmatrix} \tilde{s}(1) & \tilde{s}(2) & \cdots & \tilde{s}(N) \\ u(1) & \tilde{s}(1) & \cdot & \tilde{s}(N+1) \\ u(2) & u(1) & \cdot & \tilde{s}(N+2) \\ \vdots & \vdots & \ddots & \vdots \\ u(N_1 + N_2) & \cdots & \cdots & \tilde{s}(N-(N_1+N_2)) \end{bmatrix} \tag{2.24}$$

where $u = [u(1)u(2)\cdots u(N_1 + N_2)]^T$ is the input state vector at the beginning of the block. There are two methods to produce the set of complex path gains a_k . The first one is the Filtered Gaussian Noise Technique, where a complex uncorrelated (white) Gaussian process with a zero mean and a variance equal to one is generated in discrete time. Then, the complex Gaussian process is filtered by a Doppler filter with frequency response $H(f) = \sqrt{S(f)}$, where $S(f)$ denotes the desired Doppler power spectrum. After that, the filtered complex Gaussian process is interpolated so that its sample period is consistent with that of the input signal. The second method is sum-of-sinusoid method which is the one used in this report. Several models have been proposed for this method and they are presented

17

below.

The Clarke's Rayleigh Fading Model

The baseband signal of the normalized Clarkes two dimensional (2-D) isotropic scattering Rayleigh fading model is given by

$$a_k(t) = \frac{1}{\sqrt{N}} \sum_{n=1}^{N} exp[j(\omega_m t cos \alpha_n + \phi_n)] \tag{2.25}$$

where N is the number of the propagation path, $\omega_m = 2fv/c$ is the maximum radian Doppler frequency, v is the vehicle speed, f is the carrier frequency, and the c is the speed of light and α_n and ϕ_n are respectively, the angle of arrival and initial phase of the nth propagation path. The distributions of the α_n and ϕ_n are independent and uniform over $[-\pi, \pi)$ for all n.

The Jakes' Rayleigh Fading Model

Jakes model [19] is the simplified simulation model of Clarke's model. Since Jake's simulator needs only one-fourth the number of low-frequency oscillators as needed in Clarke's model, it is more computationally efficient. This model is a deterministic method for simulating time-correlated Rayleigh fading wave-forms. It assumes that N equal-strength rays arrive at a moving receiver with uniformly distributed arrival angles α_n, such that the ray n experiences a Doppler shift $\omega_n = \omega_m cos(\alpha_n)$, where ω_m is the maximum radian Doppler shift. Using $\alpha_n = 2\pi(n - 0.5)/N$ there is quadrantal symmetry for all Doppler shifts. As a result, the fading waveform can be modeled with $N_0 + 1$ complex oscillator, where $N_0 = N/4$. This gives

$$a_k(t) = a_C(t) + ja_S(t) \tag{2.26}$$

$$a_C(t) = \sqrt{\frac{2}{N_0}} \sum_{n=1}^{N_0} cos(\beta_n) cos(\omega_m cos(\alpha_n)t + \theta_n) \tag{2.27}$$

$$a_S(t) = \sqrt{\frac{2}{N_0}} \sum_{n=1}^{N_0} sin(\beta_n) cos(\omega_m cos(\alpha_n)t + \theta_n) \tag{2.28}$$

18

Where K is the normalization factor, α an β_n are phases, and θ_n are initial phases usually set to zero. Setting $\beta_n = \pi n/(N_0 + 1)$ gives zero cross correlation between the real and imaginary part of $T(t)$. To generate multiple uncorrelated waveforms, Jakes suggested setting the phases $\theta_{n,j} = \beta_n + 2(j - 1)/(N_0 + 1)$, where $j = 1$ to N_0 is the waveform index. However, this gives almost uncorrelated waveforms j and k only when $\theta_{n,j} - \theta_{n,k} = i\pi + \pi/2$ for some integer i; otherwise, the correlation between certain waveform pairs can be significant.

The Dent's Rayleigh Fading Model
To tackle the problem of non-zero cross correlation between imaginary and real part of the waveform, exploiting Walsh-Hadamard orthogonal vectors are suggested by Dent [13]. Then the jth waveform can be generated using

$$a_k(t) = a_C(t) + ja_S(t) \tag{2.29}$$

$$a_C(t) = \sqrt{\frac{2}{N_0}} \sum_{n=1}^{N_0} A_j(n)cos(\beta_n)cos(\omega_m cos(\alpha_n)t + \theta_n) \tag{2.30}$$

$$a_S(t) = \sqrt{\frac{2}{N_0}} \sum_{n=1}^{N_0} A_j(n)sin(\beta_n)cos(\omega_m cos(\alpha_n)t + \theta_n) \tag{2.31}$$

Where $A_j(n)$ is the jth WH code sequence in n. This gives N_0 uncorrelated waveforms, which can be efficiently generated by passing the original N_o complex oscillator values through a Fast Walsh Transform (FWT). Correlation properties are insensitive to the random number seed that is used to initialize the oscillator phases θ_n.

The Pop-Beaulieu's Rayleigh Fading Model
It was established by Pop and Beaulieu that Jakes simulator and its modifications are not Wide Sense Stationary (WSS) [37]. Meaning that its mean function $m_x(t)$ is not constant and its autocorrelation is not a function of the time difference. Pop and Beaulieu

developed a class of WSS Rayleigh fading simulators by setting $\alpha_n = 2\pi n/N$. Thus, the lowpass fading process becomes

$$a_k(t) = a_C(t) + j a_S(t) \tag{2.32}$$

$$a_C(t) = \sqrt{\frac{1}{N}} \sum_{n=1}^{N} cos(\beta_n) cos(\omega_m cos(\alpha_n)t + \theta_n) \tag{2.33}$$

$$a_S(t) = \sqrt{\frac{1}{N}} \sum_{n=1}^{N} cos(\beta_n) sin(\omega_m cos(\alpha_n)t + \theta_n) \tag{2.34}$$

However, it is mentioned in their paper that despite the WSS characteristics of this simulator, it may not model the higher order statistical properties accurately. Hence, the quality of this simulator is highly dependent on the application it is used for.

The Xiao-Zheng's Rayleigh Fading Model
Xiao and Zheng in their model proposed an improved sum of sinusoid statistical simulation model [53] and it is defined as

$$a_k(t) = a_C(t) + j a_S(t) \tag{2.35}$$

$$a_C(t) = \sqrt{\frac{1}{N}} \sum_{n=1}^{N} cos(\beta_n) cos(\omega_m cos(\alpha_n)t + \theta_n) \tag{2.36}$$

$$a_S(t) = \sqrt{\frac{1}{N}} \sum_{n=1}^{N} cos(\beta_n) sin(\omega_m cos(\alpha_n)t + \theta_n) \tag{2.37}$$

With
$$\alpha_n = \frac{2\pi n + \theta}{N} \tag{2.38}$$

Where ϕ_n, and θ_n are statistically independent and uniformly distributed over $[-\pi, \pi)$ for all n. In fact, the difference between this model and the model proposed by Pop and

Beaulieu is the introduction of random variable θ_n to the angle of arrival. In spite of decreasing the efficiency of the simulator, this model considerably enhances the statistical quality.

Li-Huangs Rayleigh Fading Model

So far, it was assumed that only one fading waveform is required. Li and Huang model [18] is able to provide multiple uncorrelated waveforms. In this model, it is supposed that M independent fading waveforms are required, each of which is composed of N sinusoids. With k^{th} fading waveform denoted by

$$a_k(t) = \sum_{n=0}^{N-1} C_{nk} e^{j(\omega_{nk} t + \phi_{nk})}, \quad k = 0, 1, \cdots, M-1 \tag{2.39}$$

where $C_n k$, ω_{nk}, and ϕ_{nk} represent the amplitude, frequency, and uniformly distributed random phase of the nth complex sinusoid in the kth fader, respectively. In addition, similar to the Jakes' model $\omega_{nk} = \omega_m cos(\alpha_{nk})$. If we assume that the incident powers are uniformly distributed and we are facing with uniform antenna gain pattern, C_{nk} can be reduced to a constant value. It is suggested to set

$$\alpha_{nk} = \frac{2\pi n}{N} + \frac{2\pi k}{MN} + \alpha_{00} \tag{2.40}$$

Where α_{00} is an initial arrival angle. By choosing the ϕ_{nk} appropriately the waveform can be expressed as

$$a_k(t) = a_{Ck}(t) + j a_{SK}(t) \tag{2.41}$$

Where

$$a_{Ck}(t) = 2C \sum_{n=0}^{N_0-1} cos(\omega_m cos\alpha_{nk} t + \phi_{nk}) \tag{2.42}$$

$$a_{Sk}(t) = 2C \sum_{n=0}^{N_0-1} sin(\omega_m cos\alpha_{nk} t + \phi'_{nk}) \tag{2.43}$$

In these equations, ϕ_{nk} and ϕ_{nk} are independent random phases uniformly distributed in $[0, 2\pi)$. $_{00}$ should be properly chosen such that asymmetrical arrival angle arrangement is ensured. In the figure 2.9, phases, and amplitudes of the $a_k(t)$ for three velocities at which receiver is moving (three different Doppler frequencies) is depicted.
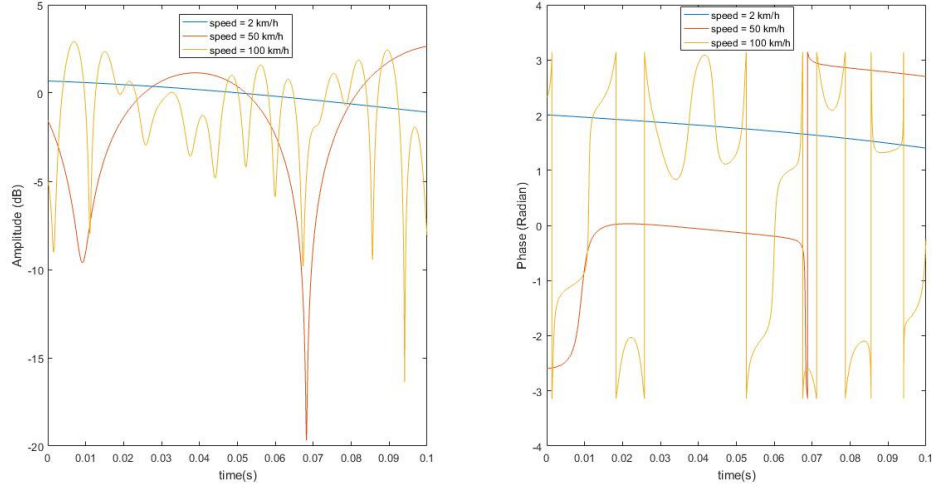
Figure 2.9: Fading channel for three values of mobile velocity

2.3.1 Simulation Results

In the figure 2.10 the performance of CSS modulation for AWGN channel and the fading are evaluated when in AWGN channel both coherent and non-coherent detection techniques are utilized. However, coherent detection technique fails in fading channel and the performance of the non-coherent detection technique is also substantially degraded. To overcome the loss of the fading channel, we are required to identify the main reason for the degradation of the CSS modulation in the fading channel. Hence, the phase and amplitude of the channel are compensated separately and together and then the performance is evaluated. Figure 2.11 shows that the major degradation is caused by the phase of the channel. Meaning that exploiting an algorithm to enhance the phase of the received signal would be highly beneficial for the performance of the system.

The effect of channel on the phase of the signal for 1 bit and 5 bits of information is illustrated in the figure 2.12 and 2.13 respectively.

22
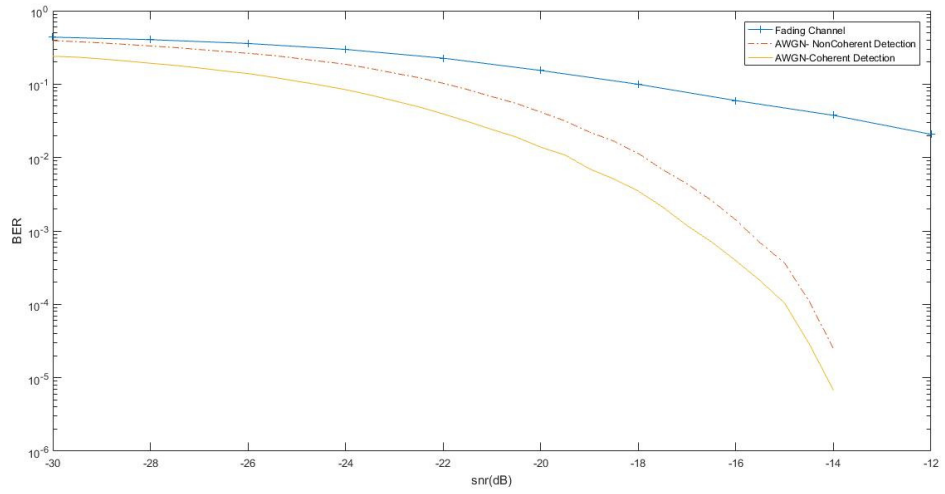
Figure 2.10: Performance of CSS modulation for Fading and AWGN channel
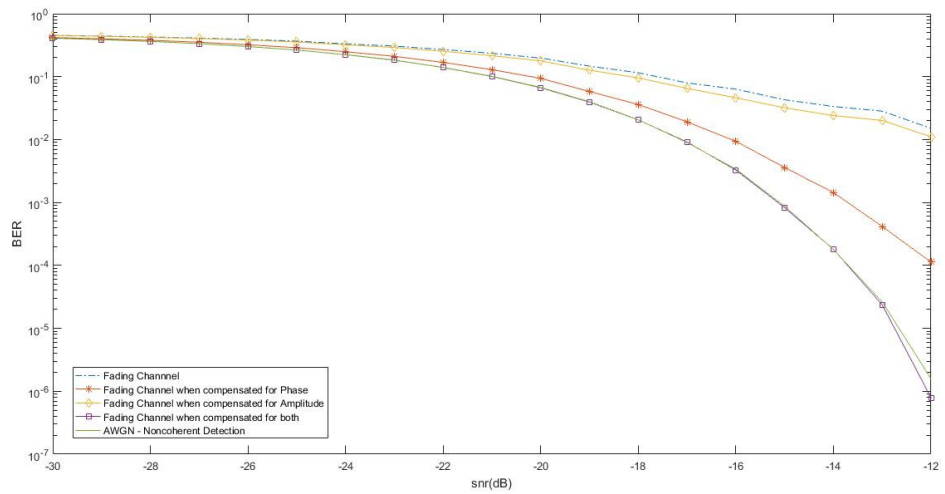
Figure 2.11: Performance of CSS in fading Channel when the effect of amplitude and/or phase is compensated

23
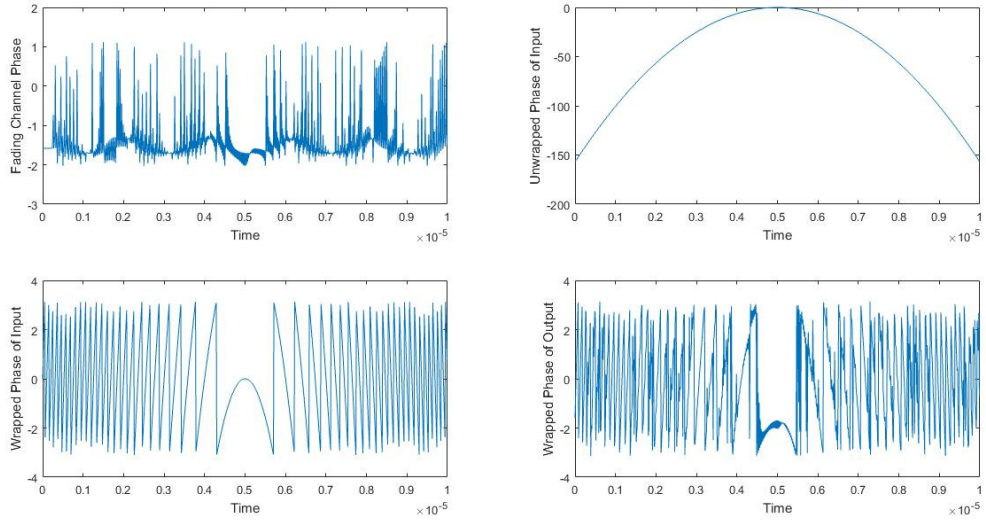
Figure 2.12: Effect of fading channel on 1-bit modulated signal
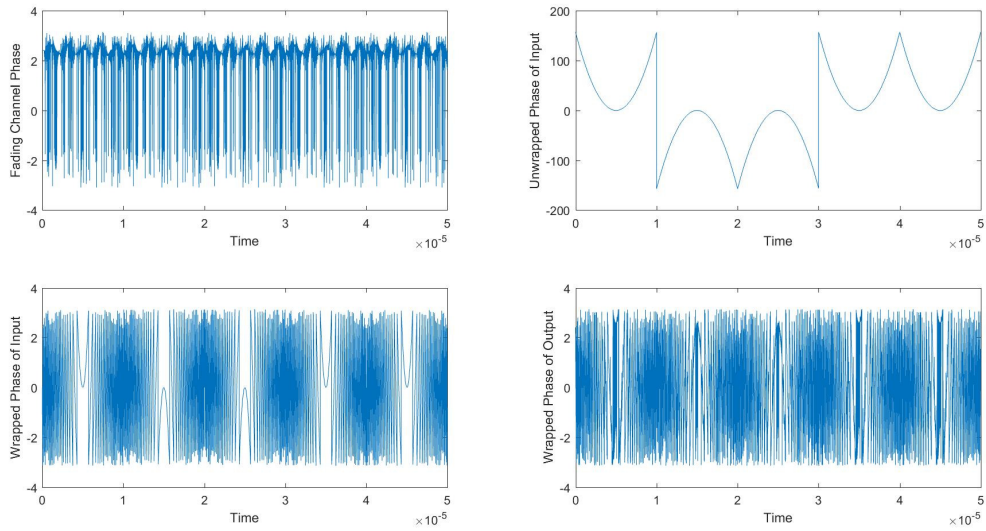
Figure 2.13: Effect of fading channel on 5-bit modulated signal

24

Superimposition in BPSK modulation

The proposed idea is to transmit the control information bits along with the data information bits while maintaining a satisfactory reliability. To compare the performance of the proposed method, a second scenario will be used as the benchmark for the comparison. In the benchmark scenario, control information is placed just before the data information and they are sent independently. Upon the successful reception of control bits, the system attempts to decode the data information bits. On the other hand, in the proposed scheme, they are sent together as without dedication of separate subframe for DCI.
The accuracy of control bits is of pivotal importance because failure in detection of these bits will lead to the failure in detection of the information data bits.

The all of the telecommunication channels, a Forward Error Correction (FEC) or channel coding technique is used to control errors of noisy and unreliable channels. The idea is to encode the message along with redundancy to allow the receiver to detect and possibly correct a limited number of errors that may occur. The noisy-channel coding theorem imposes theoretical bounds on the maximum achievable rate of the noisy channel.

The FEC codes can be divided into two separate categories based on how they work to block codes and convolutional codes. While block codes operate on a fixed sized block with a certain size, convolutional codes are able to work on an arbitrary number of bits. Convolutional codes are generally decoded by an asymptotically optimal decoding scheme at the expense of exponentially increasing the complexity. In the receiver side, block codes are usually decoded using hard-decision algorithms, it means that a hard decision is made on whether the bits are corresponding to ones or zeros. In the contrary, convolutional codes benefit from soft-decision algorithms such as the Viterbi, Message Passing Algorithm (MPA) and Bahl, Cocke, Jelinek, Raviv (BCJR) algorithms, allowing the system to have performance close to that of the Shannon limit.

In this chapter BCH codes will be used which is from the family of the blocks codes. The performance of the proposed system can be further improved by using a better FEC schemes, ideal for low rate coding schemes [16, 12, 34, 48, 49, 51, 50, 25, 24, 27]. However because the focus of this study is on the modulation technique, they are not implemented.

The BCH codes are from a class of cyclic error correcting codes constructed based on

polynomials over Galois field. In this scheme, the number of correctable errors is adjustable and it can be easily decoded with an algebraic method known as syndrome decoding.

To provide a reliable communication, control bits are assumed to have low rate encoded in a block with the length of N. The idea is to embed the control bits as a side information for the block of data bits with length N.

System Model

The total energy of the downlink is set to be unity and the ratio of the control data energy to the total energy is assumed to be r. As we will see, this ratio will be optimized to maximize the rate of the information data bits.
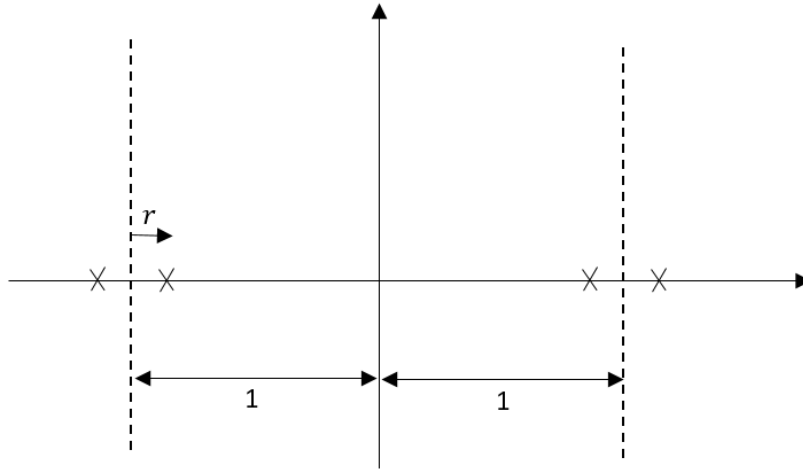
Figure 2.14: Superimposed constellation of control data and information data

Assuming an AWGN channel, the received signal is expressed as

$$Y = X + n \tag{2.44}$$

where X can be any of the four points depicted in figure 2.14, $n \sim \mathcal{N}(0, \sigma^2)$ and $\sigma^2 = N_0/2$. The detection scheme is based on hard decision, i.e. the decoder makes a definite determination each time. The detection would be such that the detector first extract the

information about the control data. It does so by determining if the received point is located on the left or right of each side of the side threshold as it is illustrated in the figure 2.14. Afterwards, it decides if it is placed on the right-side plane or on the left-side plane. The theoretical bit error probability of a BPSK system with an amplitude of magnitude A is

$$P_b = P\{y > A\} = \int_A^\infty \frac{1}{\sqrt{2\pi\sigma^2}} e^{-\frac{y^2}{2\sigma^2/2}} dy \qquad (2.45)$$

This equation can be simplified using Q-function as

$$P_b = Q(\sqrt{\frac{d_{min}^2}{2N_0}}) \qquad (2.46)$$

where $d_{min} = 2A$ in BPSK constellation and Q function is defined as

$$Q(x) = \frac{1}{2\pi} \int_x^\infty e^{x^2/2} dx \qquad (2.47)$$

In our scenario, we are dealing with a 4-point constellation. In order to understand whether we are transmitting zero or one for the control bit, we need to determine whether the received signal is on the left hand side of the either of the secondary axis or in the right hand side. For the simplicity we can assume the figure 2.15.
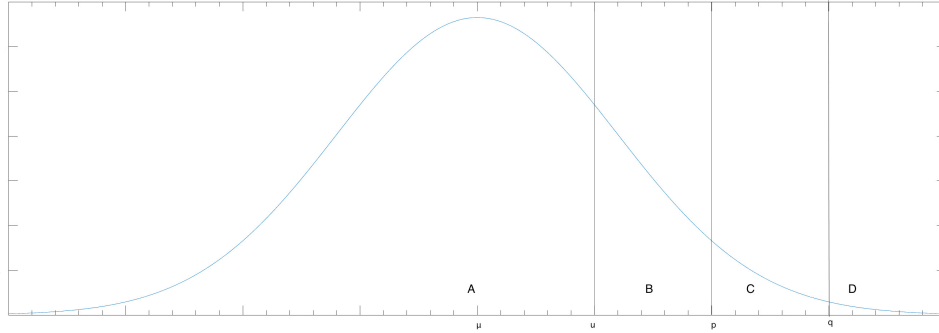
Figure 2.15: Regions of a Gaussian distribution

If the received signal is on either of the two farthest regions, error probability given the probability of the sent bit would be

$$P_e^{far} = B + D \qquad (2.48)$$

27

Otherwise, it would be

$$P_e^{near} = B + C + 2D \tag{2.49}$$

where

$$\begin{aligned}
B &= Q(\frac{\mu - u}{\sigma}) - Q(\frac{\mu - p}{\sigma}) \\
C &= Q(\frac{\mu - p}{\sigma}) - Q(\frac{\mu - q}{\sigma}) \\
D &= Q(\frac{\mu - q}{\sigma})
\end{aligned} \tag{2.50}$$

and,

$$\begin{aligned}
Q(\frac{\mu - u}{\sigma}) &= Q(\sqrt{snr}.r) \\
Q(\frac{\mu - p}{\sigma}) &= Q(\sqrt{snr}.(1 - r)) \\
Q(\frac{\mu - q}{\sigma}) &= Q(\sqrt{snr}.(2 - r))
\end{aligned} \tag{2.51}$$

All in all, the total error probability of control data can be calculated as

$$\begin{aligned}
BER_{cntrl\ data} &= \frac{1}{2}(2B + 2C + 2D) \\
&= Q(\sqrt{snr}.r)
\end{aligned} \tag{2.52}$$

Likewise, the error probability of an information data bit is

$$BER_{info.\ data} = Q((1 - r).\sqrt{snr}) \tag{2.53}$$

The accuracy of the frame of the control data is significant because its failure will result in a failure in reception of the information data block, as well. Hence, to correctly decode information data bits, correct decoding of control data is a must. It should be noted that complete reception of control data does not guarantee the accurate extraction of information data. Assuming that error correction capability of the FEC of the control data bits and information data bits are t_c and t_i, the error probability that the frame of the information data bits is decoded correctly is

$$P_f = P_f^{cntrl\ data} \cdot 1 + (1 - P_f^{cntrl\ data}) \cdot P_f^{info.\ data} \tag{2.54}$$

28

Where the $P_f^{cntrl\ data}$ is

$$P_f^{cntrl\ data} = \sum_{k=1}^{t_c} \binom{N}{k} (1 - P_b^{cntrl\ data})^{N-k} \cdot (P_b^{cntrl\ data})^k \qquad (2.55)$$

And,

$$P_f^{info.\ data} = \sum_{k=1}^{t_i} \binom{N}{k} (1 - P_b^{info.\ data})^{N-k} \cdot (P_b^{info\ data})^k \qquad (2.56)$$

It is noteworthy to mention that with the BCH coding scheme, there are only a set of acceptable t_c and t_i that we can select from. In addition, the block length of each frame should be of the form $2^m - 1$.

Optimization of the information data bit rates

Our goal is to find the maximum rate at which the information data could be transmitted while maintaining a satisfactory frame error rate. The optimization will be performed with respect to the parameters r, which is the ratio of the control signal energy to the information signal. The following iterative algorithm is used for maximizing the rate of the information data bits with the following assumptions:

- $N = 4095$

- $k_c = 31$

- $t_c = 991$

- $P_f \leq 0.01$

where N is the block length of the frame, k_c is the number of control bits to be encoded in the block, t_c is the error correction capability of the encoding scheme. Noting that the maximum rate with the fixed block length means finding the least error correction capability for information data block that satisfies the constraint on the frame error rate.

The algorithm is as follows:

Result: Finding the minimum t_i
t_i = smallest possible value; $r = 1/2$;
while $P_f > 0.01$ **do**
    Find the optimum value of r;
    if $P_f > 0.01$ **then**
        t_i = next smallest value;
    else
        break;
    end
end

Algorithm 1: Optimization algorithm

For the benchmark scenario, it is assumed that the control bits are placed just before the frame of the data, and it is modulated using the BPSK scheme. Note that, in addition to the information bits of this scenario, there exist 31 extra bits that should be accounted for. As it is illustrated in figure 2.16, The proposed method outperforms the BPSK performance for the high values of SNR.
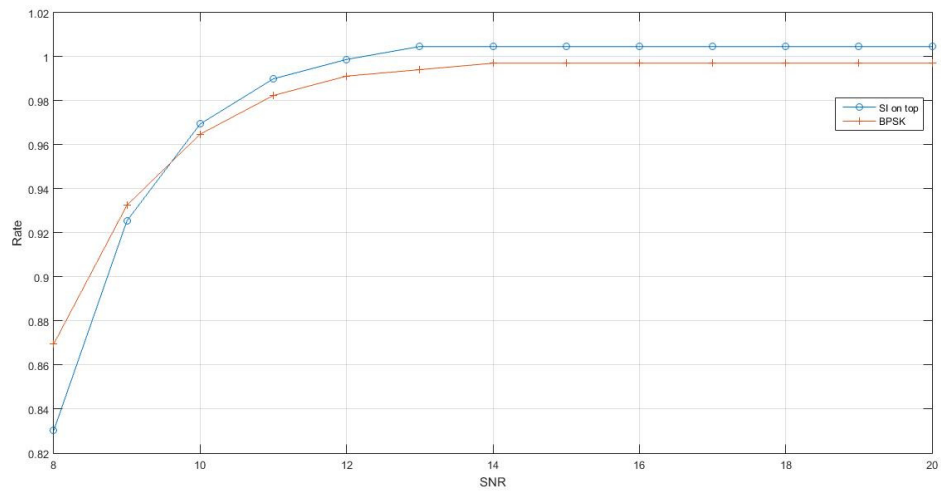
Figure 2.16: Comparing the maximized rates when using superimposed constellation and when control data are placed in the same block as information data

Chapter 3

SCMA enhancement

In this chapter, the focus is on the design of a reliable communication system with relatively high spectral efficiency. We start by going over the NOMA scheme that was proposed for the mission 5G to increase the spectral efficiency and capacity while maintaining a greater flexibility. Then, the SCMA scheme has been delineated and it will be used afterwards, to show the superiority of the presented scheme.

3.1   Background Review

NOMA is one of the approaches proposed for 5G to tackle the limitations of the preceding schemes by allowing deliberate interference in the system.LDS-CDMA is one of the proposed schemes for NOMA with code-domain multiplexing. In traditional CDMA structure, a dense spreading sequence is used to distribute the contribution of each user in each sample. The sparse spreading sequence in LDS reduces the chance of interference and lowers the complexity of detector [17]. SCMA is a generalization of LDS in which information data bits are directly mapped to an optimized constellation with multiple dimensions [30]

3.1.1 Non-Orthogonal Multiple Access

The inherent grant-based feature of LTE uplink fails to support massive connectivity with the requirement of very low latency. In addition, the grant-based procedure of LTE requires dealing with the key issues of the signaling overhead cost and the energy efficiency. For smaller packets in the uplink, the ratio of the signaling overhead to the useful payload is considerably higher; hence, the issue of overhead cost gains momentum.

While the preceding generations of communication systems exploited the FDMA in 1G, TDMA in 2G, CDMA in 3G and OFDMA for 4G, NOMA is one of the approaches proposed for 5G to tackle the limitations of the preceding schemes by allowing deliberate interference in the system. By elimination of the orthogonality requirement of LTE, NOMA will be able to achieve multiuser capacity both in uplink and downlink [11]. Being resistant to the multiuser interference is another feature of NOMA, enabling it to support longer connections with a performance near to the single user communication. Easier scheduling and link adaptation for mobile users via grant-free transmission can also be counted as the functionalities of NOMA. Based on the methods of multiplexing employed in NOMA schemes, they can be divided into two distinct categories of power domain multiplexing and code domain multiplexing [11]. In power domain multiplexing, power allocation differs from user to user, separating them depending on their channel condition. LDS-CDMA is one of the proposed schemes for NOMA with code-domain multiplexing. In traditional CDMA structure, a dense spreading sequence is used to distribute the contribution of each user in each sample. However, the sparse spreading sequence in LDS reduces the chance of interference and lowers the complexity of detector [17]. SCMA is a generalization of LDS in which information data bits are directly mapped to an optimized constellation with multiple dimensions [30]. As figure 3.1 illustrates that it can be assumed the Quadrature Amplitude Modulation (QAM) modulator and the spreader are combined to form a single unit in SCMA.
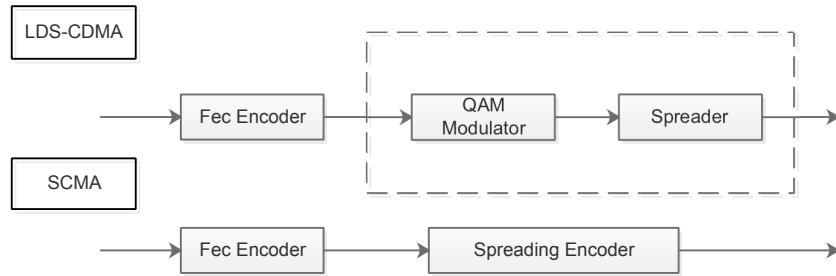
Figure 3.1: Comparing LDS-CDMA and SCMA

3.1.2   Sparse Code Multiple Access

Similar to any other coded modulations, SCMA is an generalization of the LDS-CDMA that benefits from the shaping gain [30]. A key characteristic of SCMA is the existence of a codebook set that produces a pattern for the interference of the users. Figure 3.2 is an illustration of codebook set with a codeword length of 4. In this figure, 6 layers of data, choose which codeword to transmit. Then, their transmissions are superimposed on top of each other to form an overloaded system with the overloading factor of 150%. Note that each of the cells in the figure 3.2 is a representation of an OFDMA tone. The question is how to choose a proper set of constellation points for a multi-dimensional constellation to maintain a good distance properties, as well as a maximized coding gain.
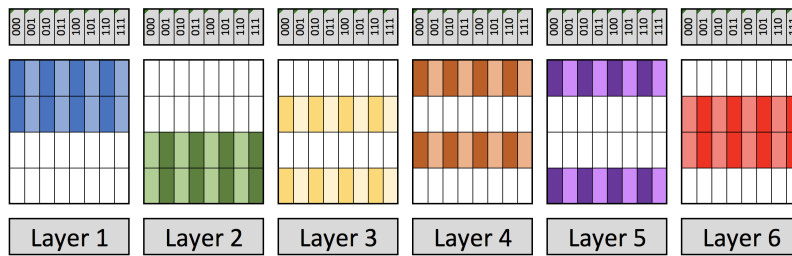
Figure 3.2: SCMA multiuser interference pattern

34

constellation design

A multi-dimensional constellation with a good performance in terms of BER or Block Error Rate (BLER) requires a large minimum distance in where no collision occurs among the layers over a single tone. In a 4-dimensional space, there exist 256 constellation points. The goal is to find a set of 16 points to maximize the minimum Euclidean distance and to impose a dependency among the complex dimensions. To reduce the complexity of the decoder, we can assume that the real and the imaginary parts of the constellations are independent. With regard to the lattice constellation principle, orthogonal QAMs on different complex planes are considered to design the mother constellation. The N-dimensional complex mother constellation can be built upon the shuffling of two N-dimensional real mother constellations which they themselves are designed based on lattice constellation. Figure 3.3 illustrates the construction of a 16-point QAM constellation from the shuffled mother construction. Furthermore, since the sum-product distance is the dominant performance indicator of high SNR ranges, an optimized unitary rotation with the angle of $(1 + \sqrt{5})/2$ is proposed to be applied to maximize the product distance [45]. Another feature of the SCMA constellation is that we are able to lower the number of projection points for the sake of the MPA decoding complexity at the cost of zeroing the minimum product distance. Layer specific operations such as phase rotation and power offset can also be defined with respect to the various system configurations.

3.1.3 Turbo Codes

A serial concatenation of codes is frequently used for power-limited systems. Reed-Solomon outer code followed by a convolutional inner code is one of the most popular schemes of concatenated codes. Turbo codes can be assumed to be a modified concatenated encoding scheme structure along with an iterative algorithm for associated code sequence. Turbo coding scheme was first introduced in 1993 by Berrou, Glavieux, and Thitimajshima [3] and shown to have a BER performance close to the Shannon limit. In this scheme, interleaved versions of the same information data bits are fed to turbo encoders in the transmitter side. In the receiver side, the soft decisions about the data sequence will be passed not only between the decoders but also from iteration to iteration to enhance the reliability. It
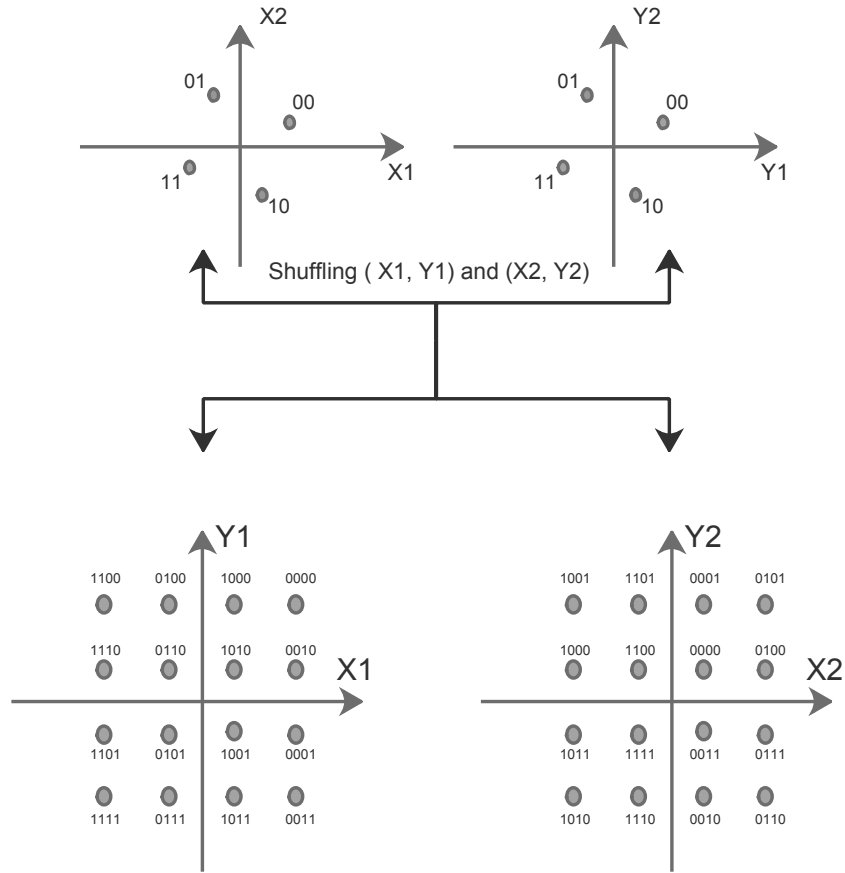
Figure 3.3: Construction of SCMA constellation

[30]

is well-known that the BER of Recursive Systematic Convolutional (RSC) codes outperform the conventional Non-recursive Systematic Convolutional (NSC) codes with the same number of memory elements M at high ranges of SNR. However, in lower SNR ranges, it is just the opposite. The turbo codes which are built upon the parallel concatenation of two RSC are able to perform better than NSC at any SNR. Moreover, puncturing can be used in turbo coding scheme for implementation of different code rates. When puncturing is used, some outputs are deleted based on the puncturing pattern in the encoder. In the receiver side, zero will be inserted in the place of deleted bits. The structures of turbo encoder and decoder are depicted in the figures 3.5 and 3.4. The Interleaver in the

36

structure of turbo codes will scatter the burst errors appearing at one of the decoders, such that the second decoder receives a sequence without burst errors. Burst errors would considerably degrade the performance of convolutional encoder and decoder because of the memory-based structure of convolutional codes.

The soft decision about the information data bits is associated with the log-likelihood ratio and they are calculated as
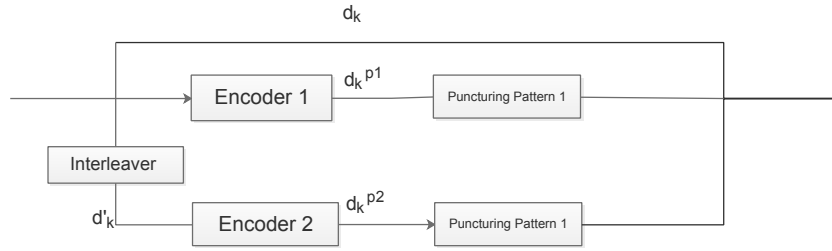
Figure 3.4: Turbo encoder structure
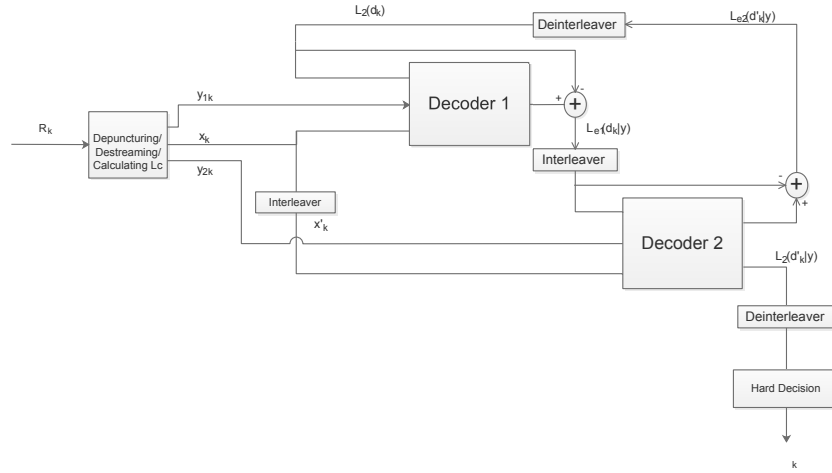
Figure 3.5: Turbo decoder structure

$$\Lambda_1(d_k) = log \frac{P_r\{d_k = 1\}}{P_r\{d_k = 0\}} \tag{3.1}$$

where $P_r\{d_k\}, i = 0, 1$ is the a posteriori probability (APP) of the information data bits d_k. Dynamic programming algorithms can be used for the optimal decoding to minimize the

error probability of the information data bits in the sequence. Viterbi algorithm which is used widely for decoding of convolutional codes cannot be used in this context because it fails to provide the A Posteriori Probability (APP) of each decoded information data bit. BCJR algorithm is a substitute algorithm than will be used to obtain the values of APP. When the RSC constraint length is K, the encoder state is

$$S_k = (a_k, a_{k-1}, \ldots, a_{k-K+1}) \tag{3.2}$$

Here, without loss of generality it is assumed that the code rate is 1/2. Hence, the information data bits sequence is assumed to be consist of N independent bits, as well as the output sequence of each convolutional encoder. After the puncturing, N bits are transmitted for systematic bits and another extra N bits will be transmitted as parity bits. In addition, the initial and the final states are set to be zero. When the modulated coded bits passed through a memoryless Gaussian channel the received sequence would be

$$R_1^N = \{R_1, R_2, \ldots, R_k, \ldots, R_N\} \tag{3.3}$$

where

$$R_k = (x_k, y_k) \tag{3.4}$$

After de-puncturing we will have

$$y_k = (y_{1k}, y_{2k}) \tag{3.5}$$

We can define a joint probability $\lambda_k^i(m)$ from which we can calculate the APP of the decoded information data bits. It can be defined by

$$\lambda_k^i(m) = P_r\{d_k = i, S_k = m | R_1^N\} \tag{3.6}$$

Thus, the APP of the decoded information data bits is equal to

$$P_r\{d_k = i | R_1^N\} = \sum_m \lambda_k^i(m), \quad i = 0, 1 \tag{3.7}$$

the Log Likelihood Ratio (LLR) of a decoded information data bit which will be then used to decide between 0 and 1 can be derived from

$$\Lambda(d_k) = log \frac{\sum_m \lambda_k^1(m)}{\sum_m \lambda_k^0(m)} \tag{3.8}$$

38

Calculation of the probability $\lambda_k^i(m)$ requires a forward backward algorithm which will be elaborated below. We define the probability functions $\alpha_k^i(m), \beta_k(m)$ and $\gamma_i(R_k, m, m')$ as

$$\alpha_k^i(m) = \frac{P_r\{d_k = i, S_k = m, R_1^k\}}{P_r\{R_1^k\}} P_r\{d_k = i, S_k = m | R_1^k\} \tag{3.9}$$

$$\beta_k(m) = \frac{P_r\{R_{k+1}^N | S_k = m\}}{P_r\{R_{k+1}^N | R_1^k\}} \tag{3.10}$$

$$\gamma_i(R_k, m', m) = P_r\{d_k = i, R_k, S_k = m | S_{k-1} = m'\} \tag{3.11}$$

Hence, the probability can be written in terms of the aforementioned probability functions as

$$\lambda_k^i(m) = \alpha_k^i(m)\beta_k(m) \tag{3.12}$$

The transition probabilities of the discrete Gaussian memoryless channel and transition probabilities of the encoder trellis determine the probability function $\gamma_i(R_k, m', m)$ as

$$\gamma_i(R_k, m', m) = p(R_k | d_k = i, S_{k-1} = m')p(d_k = i | S_k = m, S_{k-1} = m')p(S_k = m | S_{k-1} = m') \tag{3.13}$$

In addition, $\alpha_k^i(m)$ and $\beta_k(m)$ are recursively derived as

$$\alpha_k^i(m) = \frac{\sum_{m'} \sum_{i=0}^1 \gamma_i(R_k, m, m')\alpha_{k-1}^j(m')}{\sum_m \sum_{m'} \sum_{i=0}^1 \sum_{j=0}^1 \gamma_i(R_k, m', m)\alpha_{k-1}^j(m')} \tag{3.14}$$

And,

$$\beta_k(m) = \frac{\sum_{m'} \sum_{i=0}^1 \gamma_i(R_{k+1}, m', m)\beta_{k+1}(m')}{\sum_m \sum_{m'} \sum_{i=0}^1 \sum_{j=0}^1 \gamma_i(R_{k+1}, m', m)\alpha_k^j(m')} \tag{3.15}$$

To perform a recursive algorithm, the probabilities $\alpha_0^i(m)$ and $\beta_N(m)$ are initialized as

$$\alpha_0^i(0) = 1, \quad \alpha_0^i(m) = 0, \quad \forall m \neq 0, \quad i = 0, 1 \tag{3.16}$$

$$\beta_N(0) = 1, \quad \beta_N(m) = 0, \quad \forall m \neq 0 \tag{3.17}$$

From the equation 3.8 the LLR of the in information data bit d_k is derived to be

$$\Lambda_k(d_k) = log(\frac{\sum_m \sum_{m'} \sum_{j=0}^1 \gamma_1(R_k, m', m)\alpha_{k-1}^j(m')\beta_k(m)}{\sum_m \sum_{m'} \sum_{j=0}^1 \gamma_0(R_k, m', m)\alpha_{k-1}^j(m')\beta_k(m)}) \tag{3.18}$$

When we are dealing with systematic bits (x_k) the transition probabilities are meaningless, which will lead to the simplification of equation 3.18 to

$$\Lambda(d_k) = log\frac{p(x_k|d_k = 1)}{p(x_k|d_k = 0)} + log(\frac{\sum_m \sum_{m'} \sum_{j=0}^{1} \gamma_1(y_k, m', m)\alpha_{k-1}^j(m')\beta_k(m)}{\sum_m \sum_{m'} \sum_{j=0}^{1} \gamma_0(y_k, m', m)\alpha_{k-1}^j(m')\beta_k(m)}) \qquad (3.19)$$

The second part of the right-hand side equation is a function of the information produced by the encoder, namely extrinsic information$(L_e(d_k))$, has the same sign as d_k, increasing the quality of associated LLR. In the first iteration of turbo code and before the first decoder we do not have any prior information about the information data bits other than the information provided by systematic bits. When we have prior information about the information data bits, if the decoder input $(\Lambda_i(d_k) \quad for \quad i = 0, 1)$ and $(y_{ik} \quad for \quad i = 0, 1)$, the output LLR can be written as

$$\Lambda_j(d_k) = f(\Lambda_i(d_k)) + L_{je}(d_k) \quad i = 0, 1 \quad i \neq j \qquad (3.20)$$

Constraint length is also an effective factor in the performance of the turbo code. As it is investigated in [3], $K = 5$ exhibits a superior performance compared with the constraint lengths of $K = 4$ and $K > 6$. Among the generators $(G1, G2)$ for the optimum constraint length, the best results are associated with $G1 = 37$ and $G2 = 21$.

3.1.4   Iterative De-mapping

Iterative decoding idea that was proposed by turbo codes, paved the way for the application of turbo principle in other areas of communications such as soft demapping in modulation schemes. The idea of iterative de-mapping is that to use the information gained from turbo decoder to increase the reliability of de-mapping. At the receiver, the channel symbol gets demapped by log likelihood calculation of each symbol; then, the LLR of each bit is calculated accordingly. After turbo decoder, the extrinsic information which might be obtained through several iterations of the turbo decoder, will be fed back as a priori information to soft de-mapper. Figure 3.6 illustrates the block diagram of iterative de-mapper.
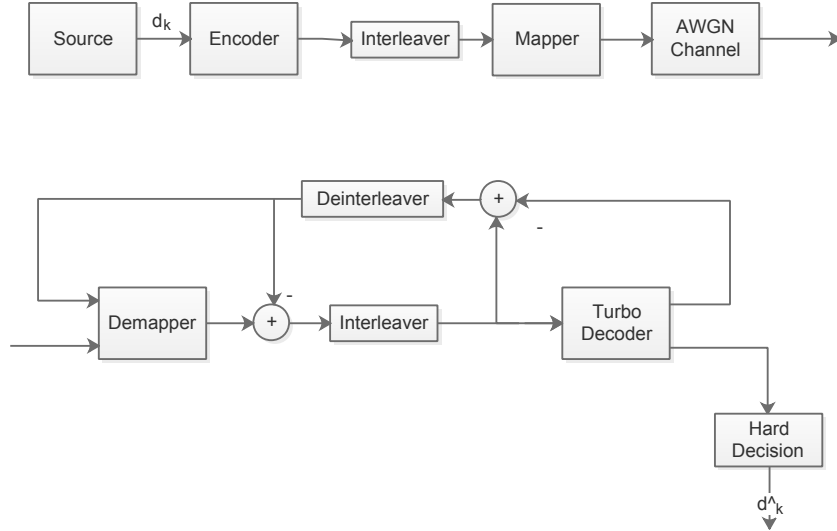
Figure 3.6: Iterative de-mapping system

Proper mapping is important for achieving a good performance. When we are dealing with non-iterative decoding systems, Gray mapping is superior, for neighboring constellation point are different only in one bit. However, it is not the case when iterative algorithms are the issue. The reason of this lies in the analysis of bit-wise mutual information [5]. Assuming $X = (X_0, \ldots, X_{M-1})$ to be the input of the memoryless Gaussian channels and Z to be the output of the channel, following relations hold for mutual information. Using this information, de-mapper updates the a posteriori values.

$$I_0 = \overline{I(X_k; Z)} = \frac{1}{M} \sum_{k=0}^{M-1} I(X_k; Z)$$

$$I_1 = \overline{I(X_k; Z|X_l)} = \frac{1}{M(M-1)} \sum_{k=0}^{M-1} \sum_{l=0l \neq k}^{M-1} I(X_k; Z|X_l)$$

$$\vdots$$

$$I_{M-1} = \overline{I(X_k; Z|\{\forall l, l \neq k\})} = \frac{1}{M} \sum_{k=0}^{M-1} I(X_k; Z|\{X \forall l, l \neq k\})$$

(3.21)

We can apply the chain rule of mutual information to get

$$I(X;Z) = \sum_{i=0}^{M-1} I_i \tag{3.22}$$

It means that symbol-based mutual information is only influenced by the SNR. When the message is passed from demapper to the decoder for the first time, there is no information available and the I_0 dominants the BER. From iteration to iteration we get more insight about the bits; thus, other terms of the $I(X;Z)$ gain the role. On the other hand, for the low values of I_0 the iterations cannot even be started due to the poor quality of reliability. Using a mapping with high I_0, i.e., the gray mapping will minimize the mutual information at no iteration. So, the iterations will not help to increase the reliability. Therefore, sacrificing some mutual information at I_0 will result in a superior performance. Figure 3.7 illustrates the relationship between the BER and I_0 with respect to the number of iterations.
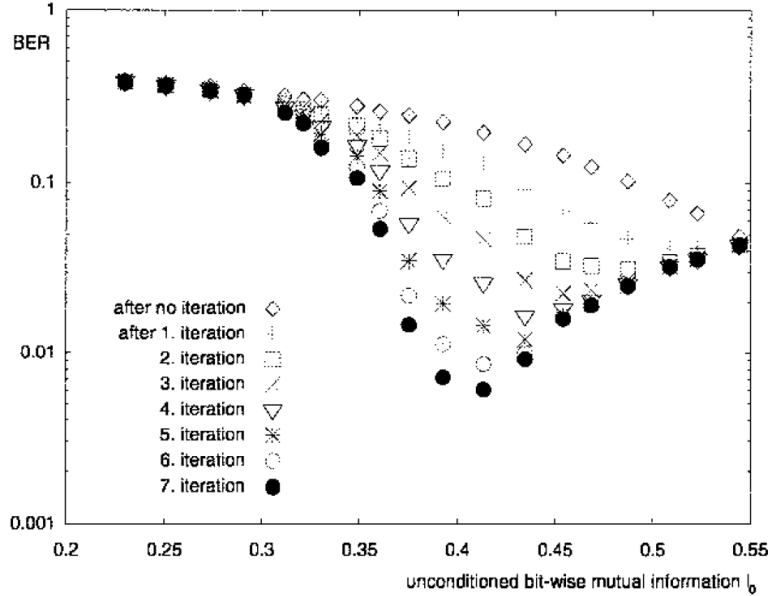

Figure 3.7: Relation between I_0 and BER, illustration from [5]

42

3.2　Set Partition Constellation Design

In this section, we tried to build a 4-dimensional constellation with a proper distance properties. This constellation can be a good candidate for the underlying structure of a communication system with high spectral efficiency. This constellation is able to transmit data bits at the rate of 1.5 bit per dimension. The design of the constellation takes advantage of the concept of set partitioning to increase the Euclidean distance between the constellation 4-dimensional constellation points. We will be using the concepts of coded modulation, Euclidean distance and set partitioning. First, the overview of these concepts has been included. Then, the design procedure will be elaborated in detail.

3.2.1　Coded Modulation

Since binary error control coding operates by inserting additional redundant symbols into the data, the required bandwidth to be used will be increased. To overcome this disadvantage, higher level modulation schemes will become useful. These modulation schemes can transmit m different symbols, each represented by different states of magnitude and phase of the carrier. Hence, in higher level modulation schemes, we are able to add redundancy by increasing the size of the signaling constellation, rather than increasing the baud rate over the channel.

From another viewpoint, it is possible to treat the coding and modulation as one entity. In the coded modulation scheme, the two stages of coding the source bits and converting the bits to modulated signals are replaced by a single process of converting the data streams directly into a signal to be transmitted. Hereby, the principle of coded modulation could be formulated as [45]:

1. Add redundancy by increasing the size of the signaling constellation

2. Combine coding and modulating processes

3.2.2 Hamming and Euclidean Distance

To design a binary code, we try to maximize the Hamming distance d_{min}, which is defined by the minimum number of digits which the two codewords differ. If a error pattern happens, the most similar codeword in the sense of having the minimum hamming distance with the erroneous stream will be used. However, in the coded modulation scheme, the actual received signal matters. Meaning that the decoder searches for a coded signal with the minimum squared error or the Euclidean distance with respect to the received. Hence, in coded modulation the minimum Euclidean distance between two coded signals are used instead of the minimum Hamming distance between two codewords.

3.2.3 Set Paritioning

In coded modulation area, the idea of set partitioning is exploited to map the points to the locations. In this method, the constellation is partitioned into two subsets of equal size, B_0 and B_1, in a way that all points in a given subset are as far apart as possible. Then, those codewords with the largest Hamming distance are used to select between points from the sets with the smallest minimum distance. This idea can be used to generate a binary label for each constellation point.

3.2.4 Set-Partition Constellation Design

In the coded modulation the processes of coding and modulating are combined together. In this design, we want to decrease the Euclidean distance between constellation points by using a certain set of signals. Meaning that, instead of using certain codewords from all possible codewords of a length, we are using specific signals instead of all possible signals in the signal set. Then, they can be coupled we a powerful channel code or it can be used in the coded modulation scheme. In this report, a 4-dimensional constellation is designed with the ability to transmit 6 bits. First, the 8 points in one dimension are partitioned into two subsets of equal size. Then, the two sets will be further partitioned in the same manner (and we will get the 4 groups of points (Figure 3.8).
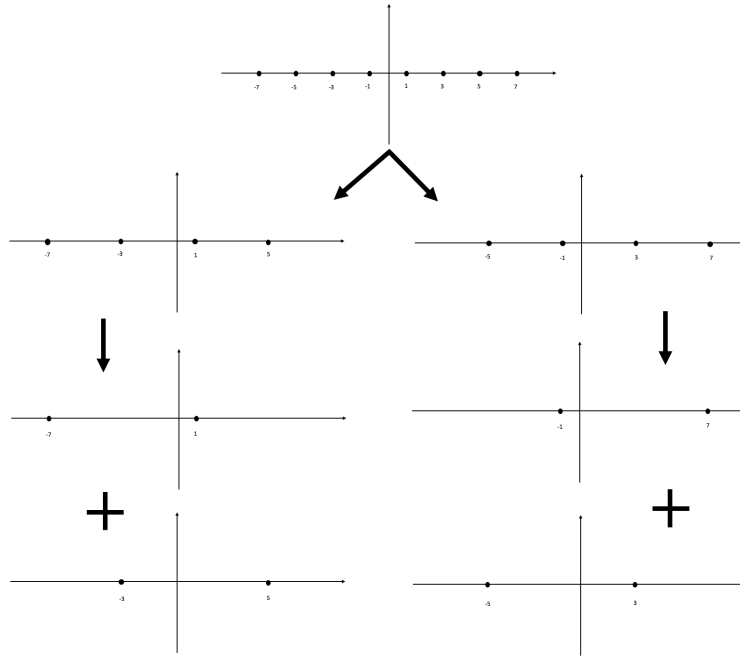
Figure 3.8: Set Partitioning of an 8-point one dimensional constellation

For the first dimension, a base ordering is selected, meaning that 2 bits are used to select a pack A, B, C, or D, and one bit specifies which point in the pack to be used in that dimension. In the second, third and fourth dimension, the ordering of the packs will be different with the purpose of increasing the minimum distance of the constellation (Figure 3.9) and the remaining bits will specify the location of their points in the pack.

The problem is how to choose a proper 4 ordering amongst all 24 possible permutations of packs. The proposed solution is a greedy algorithm that in each step in attempts to compensate by pulling apart the packs that caused the minimum distance in that step. This algorithm is as follows :

1. Select a base ordering.

2. Calculate the distances for each pair and record it in the table. Every ordering has

   - One pair at distance 7

45
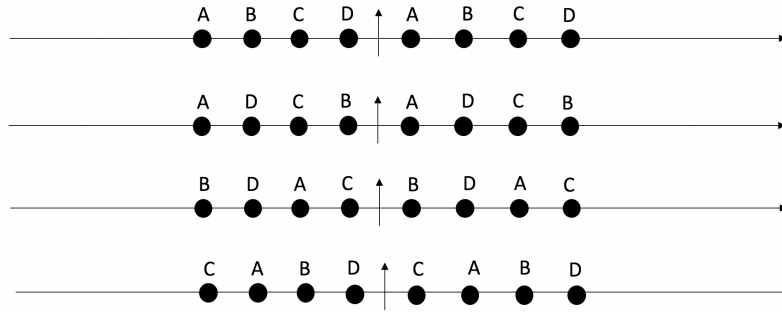
Figure 3.9: The ordeing of packs in each of the four dimensions

	Step 1		Step 2		Step 3		Step 4	
AB	5	5	7	12	6	18	5	23
AC	6	6	6	12	5	17	5	22
AD	7	7	5	12	5	17	6	23
BC	5	5	5	10	7	17	6	23
BD	6	6	6	12	5	17	5	22
CD	5	5	5	10	6	16	7	23

Table 3.1: The process of labeling in set-partition constellation

- Two pairs at distance 6
- Three pairs at distance 5

3. At each dimension Calculate the sum of the distances of previously derived order on the previous dimension.

4. Assign the distance 7 and 6 for the pairs with smallest sum distance, and 5 for the biggest. This will define one of the equivalent orderings.

5. Calculate the sum distance and move forward to the next dimension

An example sum distance table through the algorithm is given in Figure 3.1 which gives the ordering of Figure 3.9.

Constellation	Min Distance	Energy/Dimension	Bits/Dimension
8-PSK	1	1.7071	1.5
Set Partition	1	1.5	1.5
SCMA	1	0.5	1
QPSK	1	0.5	1

Table 3.2: Comparison of constellations

Table 3.2 compares the 8-Phase Shift Keying (PSK), Set partition, SCMA and Quadrature Phase Shift Keying (QPSK) Constellations. Hence, by using the proposed constellation for an equal minimum distance, less energy will be required. However, the energy needed is the same for QPSK and SCMA when a similar minimum distance is maintained.

3.3   System Model

In this report, the focus is on an uplink transmission based on NOMA scheme, such that each user may need to send data information to the base station. An additive white Gaussian noise with an average equal to zero is added to each user's data block. Each user experience a Rayleigh fading distributed according to complex Gaussian distribution with mean zero and unit variance, and it is assumed to be constant over one block of the turbo decoder. Hence, the received signal can be expressed as

$$Y = \sum_{u=1}^{U} h^u X^u + n \tag{3.23}$$

where U is the number of users transmitting in a shared channel, h^u is the channel gain of user u and n is the ambient noise. Each user may select a random or deterministic channel, i.e. an OFDMA tone, to send its data information. Therefore, in multiuser transmission, some tones may contain overlapped information data, transmitted from multiple users.

The general framework of transmitter consists of a channel allocation algorithm, a turbo encoder (as explained in 3.4) and a constellation mapper (BPSK,QPSK, 16-QAM or SCMA

constellation) and the receiver consists of demapper and turbo decoder. Some modifications might be applied for different proposed scenarios for optimizing the performance in terms of BER or BLER.

Parameter	value
Turbo Code Rate	0.5
Turbo function generators	(37-21)
Number of Turbo Iterations	3
Number of Feedback Iterations	3

Table 3.3: Simulation parameters for turbo feedback scenarios

3.4 Turbo Feedback

For the different constellations, the first step in the SCMA enhancement is to simulate a full transmitter/receiver with an AWGN channel and turbo encoder/decoder. Moreover, as explained in the introduction, it is expected that iterative demapping, i.e. a feedback to the constellation after one or some iterations of the turbo decoder, improve the performance in terms of BLER. While this technique is more effective with larger blocks, for the sake of the speed of the simulations, block lengths are mostly assumed to be 512. As the performance improves with using turbo feedback, it is implemented in all of the following simulations.

In the table 3.3, all of the default parameter values for the following simulations are provided. Any changes to this table will be noted in the corresponding simulation description.

Constellation	Energy	$MinimumDistance^2$
SCMA with any rotation	20	20
QPSK	2	2

Table 3.4: Constellation Comparison

3.5 Single User Transmission

For implementation of the SCMA technique, the 16-point SCMA constellation is examined with the minimum product distance and the shuffling multi-dimensional constellation in real and imaginary axes is proposed [30]. For a 16-point SCMA mother constellation applicable to codebooks with two non-zero elements, the proposed optimum rotation angle that maximizes the minimum product distance is

$$\arctan(\frac{1 + \sqrt{5}}{2}). \tag{3.24}$$

In the table 3.4, the SCMA constellation energy and minimum euclidean distance is calculated and compared with that of the QPSK constellation.

The BER of the uncoded SCMA versus the BER of the uncoded QPSK is plotted in the figure 3.10. Here, it is shown that the uncoded QPSK outperforms that of the SCMA.

This is verified by comparing it to the figure 5.b in the [45]. Note that the block size significantly changes the BLER, i.e., a bigger block size leads to a decreased BER. This figure also shows that the QPSK outperforms that of the SCMA in an AWGN channel.

3.5.1 Multiuser Transmission

In the multiuser scheme, a grant-free uplink will reduce the unbearable latency of LTE systems for 5G applications. Furthermore, a good spectral efficiency of the system for multiuser scenarios paves the way for massive connectivity which is one of the major specification of 5G systems.
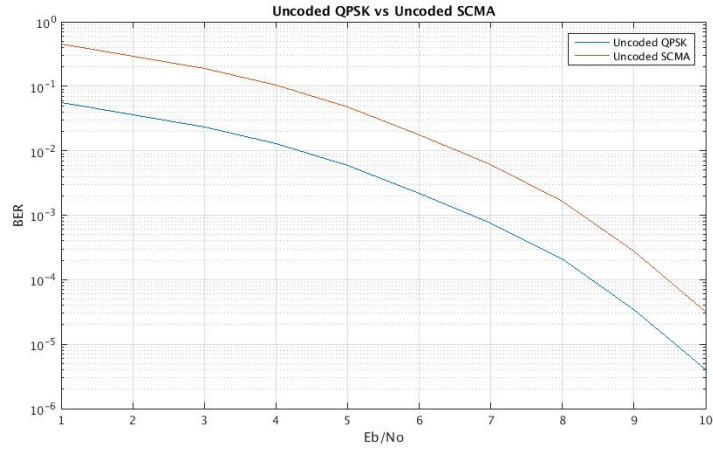
Figure 3.10: uncoded single user SCMA vs. uncoded QPSK
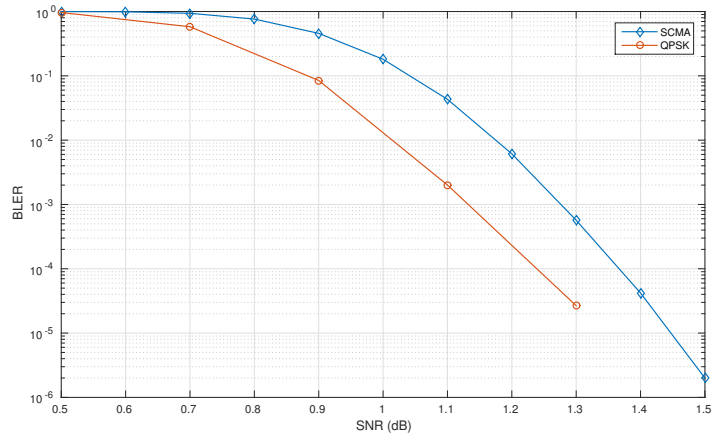
Figure 3.11: BLER of single user scheme in SCMA and QPSK in AWGN chanel

To reduce the interference, users will only transmit on some of the OFDMA tones on a pseudo-random basis at a time. Since the traffic loading, i.e., the number of simultaneous users in a time slot is not always at its peak, the real-life results will be better than the simulation results. Using a probabilistic model for the behavior of users will be beneficial as a part of future work.

Three particular scenarios have been studied to maintain the quality of the proposed system. The first scenario, which was also elaborated before, is similar to the single user transmission. In this scenario, there is no interference between the users, and each user has a dedicated channel. In the second scenario, each user selects a random channel. Hence, some interference may happen; however, the Spectral Efficiency (SE) of the system will remain the same. In the last scenario which is an extreme case, users will transmit in the single shared channel. Because of the rudimentary structure of the QPSK constellation which is used in these systems and the inherent fading which will work for us, the data information will be separable. A key point behind the system's capability to separate users is the fact that individual users are heard by the receiver through independent fading channels. In the contrary, the BLER figure shows a significant error floor in AWGN channels, due to indistinguishable points in the combined constellation. In the figure 3.12 the resulting combined constellation is depicted.
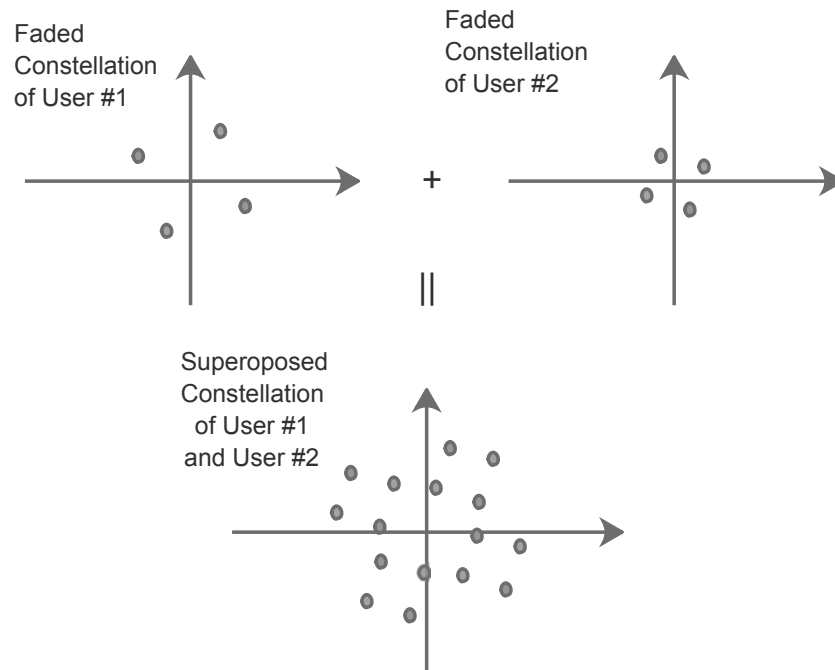

Figure 3.12: Superposition of constellations in multiuser scheme

In the receiver side, knowing that users whose data information are combined as well

as the fading channel coefficients, a super-constellation will be formed for extracting the information data bits as soft inputs for turbo decoder.

The building block of the receiver for this scenario is depicted in figure 3.13. The demapping stage will be performed using the super-constellation, such that the soft inputs are fed to the turbo decoders of each user. Therefore, unlike the successive decoding, the proposed joint decoding will be able to output the decoded bits simultaneously, satisfying the low latency requirements of 5G. Then, depending on the successful decoding of the information data bits of each user, the super-constellation will be refined to be a simpler one, i.e. the superposition of the constellation of the failed users. Then the iterative demapping will enhance the quality of soft inputs;. The aforementioned steps will be pursued again as the second feedback iterations. The turbo decoder of each user may perform turbo decoding for several iterations for achieving a superior quality estimation of the information data bits.
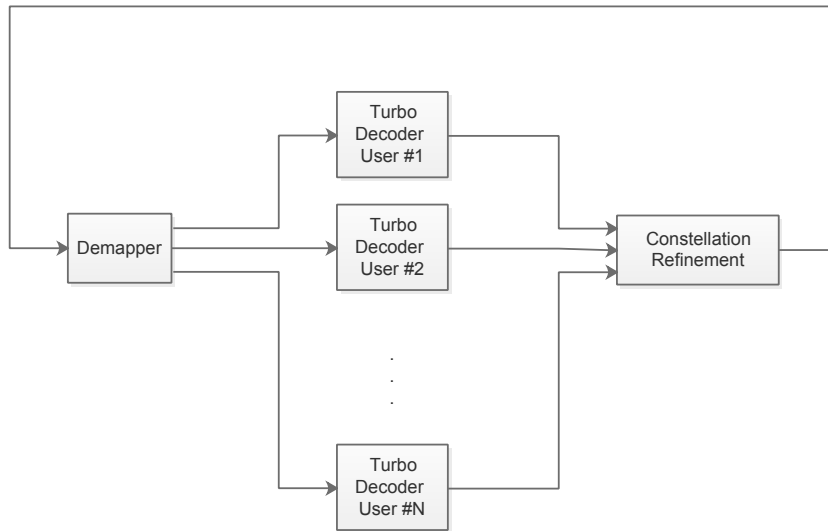

Figure 3.13: Receiver of multiuser turbo decoder

The figure 3.16 illustrates the difference between the SCMA constellation and the QPSK constellation when they are used in the multiuser scenarios. It is proved that QPSK outperforms the SCMA constellation, because of the simple structure of the constellation with the similar minimum distance properties to that of theSCMA. In addition, QPSK

benefits from Gray mapping, while it is not the case for SCMA constellation because of its complex structure.
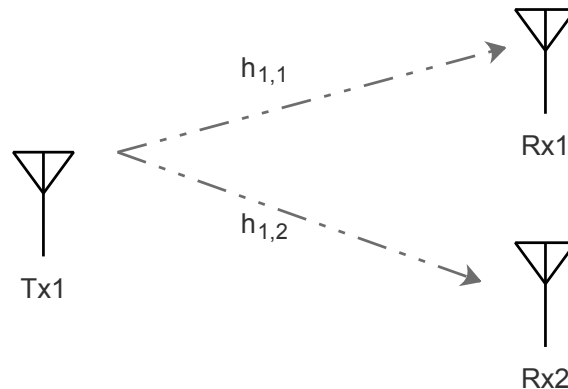

Figure 3.14: Multi Antenna Scheme

To conquer the destructive effect of a fading channel, we can use a multi antenna system in a receiver. One primary reason to use multiple antennas is to improve link quality and reliability. For example, a basic form of a receiver is consists of two antennas at a certain distance from each other, and because of the difference in physical location, each receives a slightly different version of the sent signal. The receiver mathematically combines them to form a better estimate of the transmitted signal compared with the situation where it had only one receive antenna[44]. This technique is also called spatial diversity because the receiver antennas are spatially separated from each other. We can see in the figures 3.17 and 3.18 that a multi-antenna scheme is able to improve the performance of the system significantly. In addition, it is shown in figure 3.17 that proposed system will also outperform SCMA in the multi-antenna scheme.
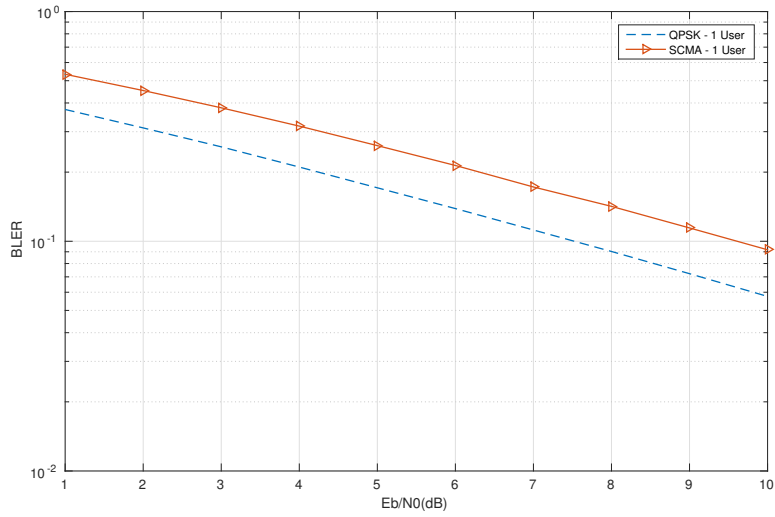
Figure 3.15: Receiver of the single-user turbo decoder

Figure 3.16: Receiver of the multi-user turbo decoder when the users select random tones for transmission (random overlap) and when the users select the same tones (always overlap).
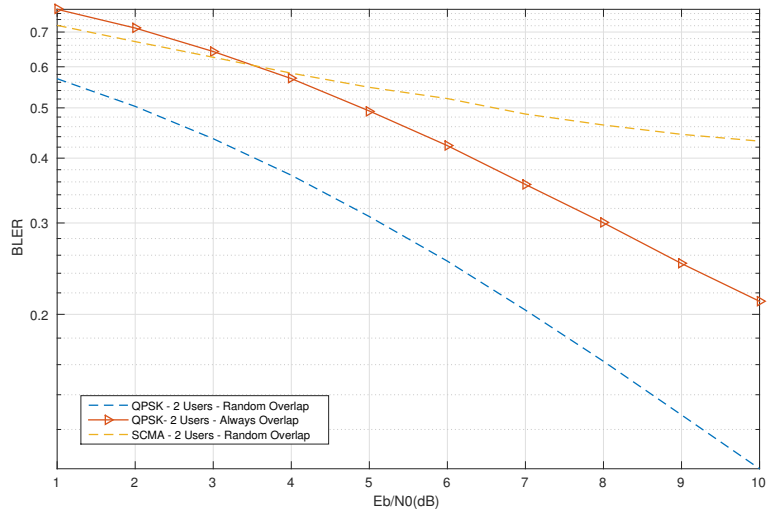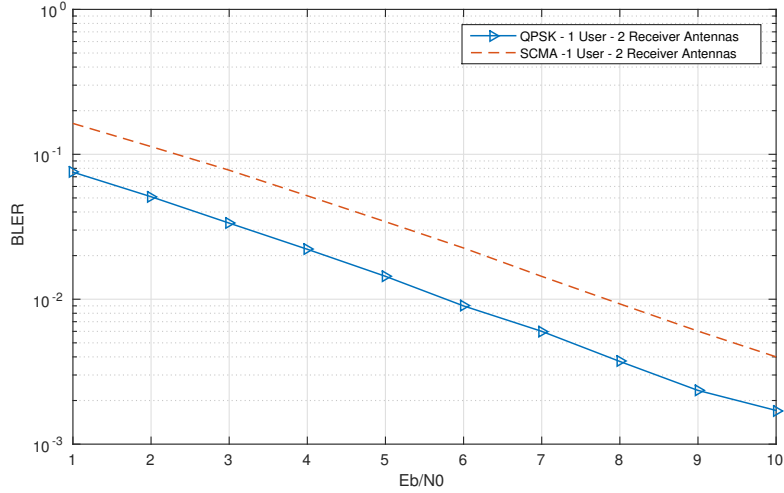
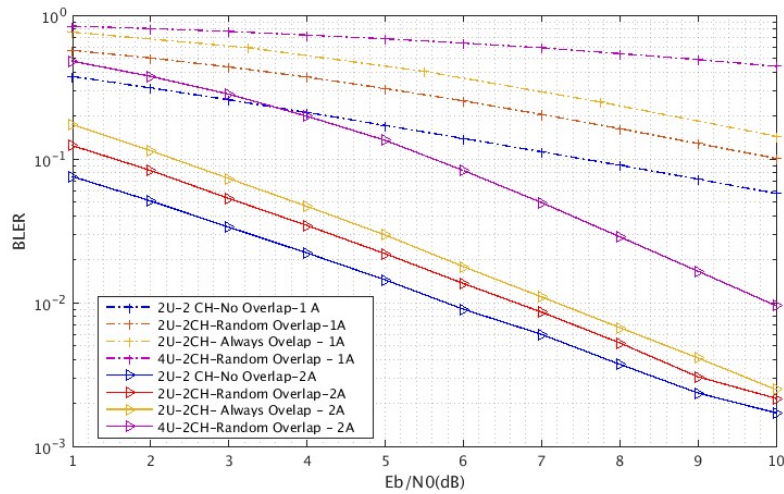Figure 3.17: Receiver of the multi-user turbo decoder

Figure 3.18: Receiver turbo decoder when the users select separate tones, random tones and the same tones for transmission(U, CH, A reperesent user,channel and antennas respectively)

Chapter 4

Conclusion

In this thesis, we have proposed a grant-free scheme for transmission of control and data signals over shared time/frequency resources by exploiting the potentials of spread spectrum communication systems. We have used a chirp signal, to use the entire allocated bandwidth for broadcasting the signal. The inherent capability of interference attenuation of chirp signal helped us to transmit both data and control signals on top of each other with a minimal degradation of the performance.

Because of the long duration of chirp signals, we need to use the fast fading channel for simulation purposes. Many different techniques have been proposed in the literature to simulate the fading channels. Basically, they generate uncorrelated fading waveforms to be used for the modeling of the frequency selective fading channels. Each model is able to successfully model the channel for some specific applications while having drawbacks that make it unusable for the others. We have used the sum-of-sinusoid method for simulating the fast fading channel.

In addition, a NOMA scheme is used in conjunction with turbo codes. In turbo codes, two or more component codes are used concurrently, and decoding involves feeding outputs from one decoder to the inputs of other decoders in an iterative fashion. In fact, the soft information on data bits passed between the components of the turbo codes; then, they would be fed back again in the beginning to increase the reliability of the decisions. We have used the iterative notion of turbo codes for efficient decoding of multiuser scheme in

a slow fading channel. We have shown the performance of the proposed scheme is able to outperform the performance of the SCMA scheme. The rationale behind this is the fact that, the simple constellation of our scheme - QPSK - can tolerate the superposition of constellations. It addition, QPSK is taking advantage of gray coding, while it is not the case for the SCMA constellation.

References

[1] 5G; Study on scenarios and requirements for next generation access technologies (3GPP TR 38.913 version 14.2.0 Release 14). Technical report, 2017.

[2] Sueng Jae Bae, Young Min Kwon, Mi-young Lee, Bon Tae Koo, and Min Young Chung. Femtocell interference analysis based on the development of system-level LTE simulator. *Wireless Communications and Networking*, pages 1–18, 2012.

[3] Claude Berrou, Alain Glavieux, and Punya Thitimajshima. Near optimum error correcting coding and decoding: turbo codes. *IEEE Transactions on Communications*, 44(10):1261–1271, 1996.

[4] Joseph Boutros, Emanuele Viterbo, Catherine Rastello, and Jean-Claude Belfiore. Good lattice constellations for both Rayleigh fading and Gaussian channels. *IEEE Transactions on Information Theory*, 42(2):502–518, 1996.

[5] Stephan Brink, Joachim Speidel, and Ran-Hong Yan. Iterative demapping and decoding for multilevel modulation. 1998.

[6] Stephan Ten Brink. Convergence behavior of iteratively decoded parallel concatenated codes. *IEEE Transactions on Communications*, 49(10):1727–1737, 2001.

[7] A.G Burr. Block versus trellis: an introduction to coded modulation. *Electronics & Communication Engineering Journal*, 5(4):240–248, 1993.

[8] Yunlong Cai, Zhijin Qin, Fangyu Cui, Geoffrey Ye Li, and Julie A Mccann. Modulation and Multiple Access for 5G Networks. pages 1–31, 2017.

[9] Philip A. Catherwood and William G. Scanlon. Ultra-wideband communications - An idea whose time has still yet to come? *IEEE Antennas and Propagation Magazine*, 57(2):38–43, 2015.

[10] By R H Clarke. A statistical theory of mobile-radio receptions. *The Bell System Technical*, 47(6):957 – 1000, 1968.

[11] Longlong Dai, Bichai Wang, Yifei Yuan, Shuangfeng Han, Chih-Lin I, and Zhaocheng Wang. Non-orthogonal multiple access for 5G : solutions , challenges , opportunities , and future research Trends. *IEEE Communications Letters*, 53(9):74–81, 2015.

[12] Armin Dekorsy, Volker Kuehn, and Karl-dirk Kammeyer. Low-rate channel coding with complex valued block codes. *IEEE Transaction on Communications*, 51(5):800–809, 2003.

[13] P Dent, G E Bottomley, and T Croft. Jakes fading model revisited. *Electronics Letters*, 29(13):1162–1163, 1993.

[14] Pal Frenger, Pal Orten, and Tony Ottosson. Code-spread CDMA using maximum free distance low-rate convolutional codes. *IEEE Transactions on Communications*, 48(1):135–144, 2000.

[15] J. Hagenauer. Forward error correcting for CDMA systems. *International Symposium on Spread Spectrum Techniques and Applications*, 2(3):566–569, 1996.

[16] J Haghighat and H Jamali. High perfomance LDPC codes for CDMA applications. *Mobile and Wireless Communication Network*, pages 105–109, 2002.

[17] Reza Hoshyar, Ferry P Wathan, and Rahim Tafazolli. Novel low-density signature for synchronous CDMA systems over AWGN channel. *IEEE Transactions on Signal Processing*, 56(4):1616–1626, 2008.

[18] Xiaojing Huang and Yunxin Li. The generation of Iindependent rayleigh faders. In *IEEE Conference on Communications*, pages 41–45, New Orleans, LA, USA, 2000. IEEE.

[19] William C Jakes. *Mobile radio systems*. Wiley-IEEE Press, 1974.

[20] Y.~M. Kim and B.~D. Woerner. Comparison of trellis coding and low rate convolutional coding for CDMA. *Military Communication Conference*, pages 765–769, 1994.

[21] Stéphan Lefrancois and David Haccoun. Search procedures for very low rate quasi-optimal convolutional codes. *IEEE International Symposium on Information Theory - Proceedings*, page 278, 1994.

[22] M. Lentmaier and K. Sh Zigangirov. On generalized low-density parity-check codes based on Hamming component codes. *IEEE Communications Letters*, 3(8):248–250, 1999.

[23] F. Li and H. Imai. An overview of forward error-correction coding for spread spectrum. *Proceedings International Symposium on Spread Spectrum Techniques and Applications*, pages 1193–1197, 1996.

[24] Kai Li, Xiaodong Wang, Guosen Yue, and Li Ping. A low-rate code-spread and chip-interleaved time-hopping UWB system. *2006 IEEE Conference on Information Sciences and Systems, CISS 2006 - Proceedings*, 24(4):609–614, 2006.

[25] Gianluigi Liva, Balázs Matuz, Enrico Paolini, and Marco Chiani. Short low-rate non-binary turbo codes. *International Symposium on Turbo Codes and Iterative Information Processing*, (1):41–45, 2012.

[26] Stephaa Maqois and David Haccoun. Very low Rate quasi-optimal convolutional codes for CDMA. *Canadian Conference on Electrical Engineering*, pages 210–213.

[27] Balazs Matuz, Gianluigi Liva, Enrico Paolini, Marco Chiani, and Gerhard Bauch. Low-rate non-binary ldpc codes for coherent and blockwise non-coherent awgn channels. *IEEE Transactions on Communications*, 61(10):4096–4107, 2013.

[28] J J Maxey and R F Ormondroyd. Low-rate orthogonal convolutional coded DS-CDMA using non-coherent multicarrier modulation over the awgn and rayleigh faded channel. *International Symposium on Spread Spectrum Techniques and Applications*, pages 575–579, 1996.

[29] Scott L. Miller. Design and analysis of trellis codes for orthogonal signal sets. *IEEE Transactions on Communications*, 43(2 -4 pt 2):821–827, 1995.

[30] Hosein Nikopour and Hadi Baligh. Sparse code multiple access. pages 332–336, 2013.

[31] R F Ormondroyd and J J Maxey. Performance of low rate orthogonal convolutional codes in DS-CDMA. *IEEE Transactions on Vehicular Technology*, 46(2):320–328, 1997.

[32] Raymond L. Pickholtz, Donald L. Schilling, and Laurence B. Milstein. Theory of spread-spectrum communications-A tutorial. *IEEE Transactions on Communications*, 30:855–884, 1982.

[33] Li Ping, Xiaoling Huang, and Nam Phamdo. Zigzag codes and concatenated zigzag codes. *IEEE Transactions on Information Theory*, 47(2):800–807, 2001.

[34] Li Ping, W K Leung, and K Y Wu. Low-rate turbo-hadamard codes. *IEEE Transactions on Information Theory*, 49(12):3213–3224, 2003.

[35] Li Ping, Lihai Liu, K. Y. Wu, and W. K. Leung. Approaching the capacity of multiple access channels using interleaved low-rate codes. *IEEE Communications Letters*, 8(1):4–6, 2004.

[36] Li Ping, Lihai Liu, Keying Wu, and W. K. Leung. On interleave-division multiple-access. *IEEE Transactions on Wireless Communications*, 5(4):938–947, 2006.

[37] Marius F Pop and Norman C Beaulieu. Limitations of sum-of-sinusoids fading channel simulators. *IEEE Transactions on Communications*, 49:699–708, 2001.

[38] Chinmay Rao and Ram M Narayanan. Spectral efficiency considerations in ultrawideband (UWB) radar and communications. *Measurement*, 5820:224–234, 2005.

[39] Himanshu Saraswat, Govind Sharma, Sudhir Kumar Mishra, and Vishwajeet. Performance evaluation and comparative analysis of various concatenated error correcting codes using BPSK modulation for AWGN channel. *International Journal of Electronics and Communication Engineering*, 5(3):235–244, 2012.

[40] I. Song and B. Woerner. Combined coding and modulation for wireless communication using multidimensional PSK signal constellations. *Military Communication Conference*, 3:1023–1027 vol.3, 1993.

[41] Vladislav Sorokine, Frank R Kschischang, and Subbarayan Pasupathy. Innovative coding scheme for spread-spectrum communications. *International Symposium on Personal, Indoor and Mobile Radio Communications*, pages 1491–1495, 1998.

[42] Vladislav Sorokine, Frank R. Kschischang, and Subbarayan Pasupathy. Gallager codes for CDMA applications-Part II: implementations, complexity, and system capacity. *IEEE Transactions on Communications*, 48(11):1818–1828, 2000.

[43] Nuno Souto, Joao Carlos Silva, Francisco Cercas, Americo Correia, and Antonio Rodrigues. Low rate convolutional and turbo codes based on non-linear cyclic codes. *Wireless Communications and Mobile Computing*, 7(1):23–34, 2007.

[44] Andrej Stefanov and Tolga M. Duman. Turbo coded modulation for wireless communications with antenna diversity. *Journal of Communications and Networks*, 2(4):356–360, 2000.

[45] Mahmoud Taherzadeh, Hosein Nikopour, Alireza Bayesteh, and Hadi Baligh. SCMA codebook design. 2014.

[46] William H Tranter, K Sam Shanmugan, Theodore S Rappaport, and Kurt L Kosbar. *Principles of communication systems simulation with wireless applications*. Prentice hall, 2003.

[47] David Tse and Pramod Viswanath. *Fundamentals of wireless communication*. 2005.

[48] Andrew J Viterbi. Spread spectrum communications–Myths and realities. *IEEE Communications Magazine*, 17(3):11–18, 1979.

[49] Andrew J. Viterbi. When not to spread spectrum: A sequel. *IEEE Communications Magazine*, 23(4):12–17, 1985.

[50] Andrew J. Viterbi. Very low rate conventional codes for maximum theoretical performance of spread-spectrum multiple access channels. *Selected Areas in Communications*, 8(4):641–649, 1990.

[51] Andrew J. Viterbi. Very low rate convolutional codes for maximum theoretical performance of spread-spectrum multiple-access channels. *IEEE Journal on Selected Areas in Communications*, 8(4):641–649, 1990.

[52] Yige Wang and Marc Fossorier. Doubly generalized LDPC codes over the AWGN channel. *IEEE Transactions on Communications*, 57(5):1312–1319, 2009.

[53] Chengshan Xiao, Yahong Rosa Zheng, and Norman C Beaulieu. Novel sum-of-sinusoids simulation models for Rayleigh and Rician fading channels. *IEEE Transactions on Wireless Communications*, 5(12), 2006.

[54] Guosen Yue, Li Ping, and Xiaodong Wang. Generalized low-density parity-check codes based on Hadamard constraints. *IEEE Transactions on Information Theory*, 53(3):1058–1079, 2007.